Hosting capacity in power systems considering seasonal and hourly capacity ratings for the transmission lines, under sufficiency criterion

By

Jorge Andrés Pérez Martínez

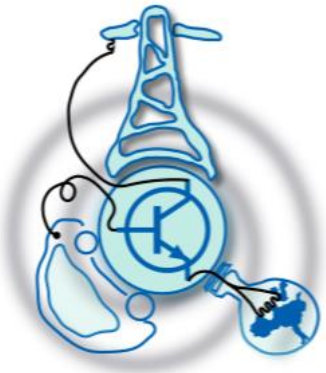

Submitted to the Department of Electrical Engineering, Electronics, Communications and Systems
In partial fulfillment of the requirements for the degree of
Erasmus Mundus Joint Master Degree in
Sustainable Transportation and Electrical Power Systems – STEPS
at the
UNIVERSIDAD DE OVIEDO
August 2024

Autor.....Jorge Andrés Pérez Martínez

Certified by.....Rui Pestana
Advisor – Rede Eléctrica Nacional, S.A. (REN)
Thesis supervisor

Certified by.....Cristina Isabel Faustino Agreira
Associate Professor – Instituto Politécnico de Coimbra
Thesis supervisor

Hosting capacity in power systems considering seasonal and hourly capacity ratings for the transmission lines, under sufficiency criterion

By

Jorge Andrés Pérez Martínez

Submitted to the Department of Electrical Engineering, Electronics, Communications and Systems
On August 26th, 2024, in partial fulfillment of the requirements for the degree of
Erasmus Mundus Joint Master Degree in
Sustainable Transportation and Electrical Power Systems – STEPS

Abstract

When considering the operation of transmission networks in the medium and long term, it is necessary to determine the amount of additional power that each node of the network can allocate. This aspect is intrinsically related to the transport capacity of the transmission lines in the network, which consequently requires more precise estimates of this transport capacity for medium and long term operational and planning studies. This work proposes the use of more accurate estimates, without reaching real-time estimates, of the transmission capacity. The objective is to determine the amount of additional power that a transmission network node can accommodate without requiring additional investment in transmission infrastructure. This capacity is determined using a representative sample of system operating conditions, followed by a steady-state contingency analysis to quantify the expected amount of network congestion caused by the addition of a new generation facility. The main result of the design and implementation of the methodology is the value of additional power that each node in the grid can accommodate, comparing the impact of using three different transmission capacity estimates, Static Line Rating (SLR), Seasonal Adjustment Rating (SAR), and Ambient Adjustment Rating (AAR).

Keywords: hosting capacity, seasonal adjustment rating, ambient adjusted rating, N-1 condition.

Thesis Supervisor: Rui Pestana
Title: Advisor – Rede Eléctrica Nacional, S.A. (REN)

Thesis Supervisor: Cristina Isabel Faustino Agreira
Title: Associate Professor – Instituto Politécnico de Coimbra

Acknowledgement

To my mother, Orfilia, a never-ending source of love, support, and sacrifice. Your words of encouragement and confidence have been my driving force to achieve this goal. Thank you for believing in me and for being my inspiration and support in every step of this academic journey.

To my beloved family, for your unwavering support at all times. Thank you for understanding the absences and sacrifices necessary to dedicate myself to this program and research. Your trust and affection have been my pillar in this journey.

To my thesis advisors, Rui and Cristina, for your expert guidance, patience, and dedication. Your advice and constructive comments were instrumental in shaping this research. Both were willing to listen and provide guidance throughout the process of developing this thesis.

To my brother by choice, Luis, your unconditional support and sincere friendship have sustained me throughout this challenging journey. You have always been there to listen to my concerns, to encourage me in difficult times, and to celebrate successes with me.

To my friends, for your encouragement, laughter, and support during the most challenging moments. Your friendship has made this journey more enjoyable and meaningful. I am grateful for the advice and knowledge you have shared with me along the way.

To my mentors and teachers, for your expert and dedicated guidance. Thank you for sharing your knowledge and experience and for giving me the opportunity to grow academically and personally. Your teachings have been invaluable to my education.

To all the people who have contributed in one way or another to this process, my deepest thanks. Each of you has been an important part of this achievement, which I celebrate with emotion and gratitude.

Jorge A. Pérez.

Table of contents

List of figures

List of tables

1 Introduction

1.1 Background

In the context of the growing demand for electric power and the increasing incorporation of renewable energy sources, the evaluation of hosting capacity in power systems has become a crucial challenge. The transport capacity of transmission lines plays a fundamental role in system efficiency and reliability but is subject to various environmental conditions and operational settings. The present research arises from the need to understand how seasonal and hourly adjustments can affect the transport capacity of transmission lines, and how these variations can influence the hosting capacity for different generation technologies. Through this study, we seek to contribute to the optimization and planning of electrical systems, allowing better integration of renewable sources and guaranteeing a sustainable and secure electrical supply in medium and long-term horizons.

This work focuses on using power flows to determine whether a transmission network suffers from overloads as a consequence of incorporating generation at a system node. This is done without considering additional expansions in the transmission network. A sample that represents the typical annual operation of an electrical system is used, so that the possible changes to the operation due to natural variations in demand and the effect of variable renewable generation, which has a greater impact on electrical systems, can be captured. Within this analysis, the N-1 criterion was considered, so that it is possible to identify the sufficiency of the network in the event of adverse conditions such as the unavailability or failure of one of its elements, without compromising the integrity of the operation and the system infrastructure.

1.2 Objectives

The main idea of this work was to identify a mechanism that would allow knowing, at least in a preliminary form, the capacity of a transmission node to accommodate additional power, without the transmission network being a constraint to the operation. This would include the effect of environmental adjustments on the transport capacity of transmission lines.

By simulating the operational conditions of a system, additions to the generation park were made in incremental steps to subsequently evaluate the power flow in the network under normal and single contingency conditions. The

simulation was performed using the aforementioned adjustments to the capacity of the transmission lines.

The simulation of power flows was performed on a representative sample of the annual operation of an electrical system so that the operational limits of the transmission lines are respected. For a node to be able to allocate the power, it is expected that it will not cause overloads in an acceptable percentage of hours during the year. Overloads in the transmission network generally require remedial actions, which in this context consist of reductions in plant's output. The curtailment of the power plants can cause excess costs to the system since the system must pay compensation to the generating agents, as their participation in the electricity market is limited for reasons beyond their control.

Consequently, the first objective of the study is to provide a scalable and adaptable tool to identify indicatively the hosting capacity of a transmission node. This is intended to serve as input for the planning of additions to the generation park in medium and long-term horizons, as well as to serve as input for the opinion of interconnection permits for producing agents under the premises of free access to the transmission network.

The second objective of the study is to quantify the effect of using adaptive capacities of transmission lines on the capacity of nodes to accommodate additional power. This would allow for the mitigation of dispatch restrictions in the transmission network without making investments in infrastructure since this requires minor investments in improving models and updating information on the average ambient conditions of the environment.

1.3 Thesis structure

The report follows a simple and straightforward structure, without reducing the rigor required for an analysis of this type. The structure of the report is as follows:

1.3.1 Chapter 1: Introduction

A brief description is provided as a general overview of the project, its scope and objectives. As well a mention of the technical motivations and possible needs that the results of this work can cover.

1.3.2 Chapter 2: Literature review

A theoretical summary of the concepts necessary for the analysis presented is provided. The calculation of transmission line transport capacity and the effect of environmental conditions on this value are detailed. Also described are the

seasonal adjustments and adjustments based on environmental conditions to the transmission capacity, based on the guidelines of international regulatory bodies.

A summary of criteria used for the planning of generation additions is presented. This is from the perspective of the inclusion of new plants without requiring major changes in the network topology. Finally, aspects of operational safety and sufficiency in transmission are mentioned, which are necessary to identify compliance with quality and safety criteria in the electric power system.

1.3.3 Chapter 3: Methodology

This section provides a detailed description of the design of the methodology and the criteria and reasoning used for it. The information used as a basis for constructing the operating scenarios that represent the annual operation is described. The transmission network model used for the tests and the method used to incorporate the base generation and demand information into the reduced transmission network model is detailed.

The adjustments made to the transmission capacity are also described. Initially, the seasonal adjustment is detailed with a single factor for each month of the year, and then the resolution is increased using an hourly factor for each month according to the environmental conditions considered for each case.

Then, the construction of the scenarios in the PSS®E model is detailed, as well as the modelling options selected for voltage control, dispatching of the existing units and the numerical solution algorithm used. Finally, the operational safety criteria and other general considerations for the simulation are detailed.

1.3.4 Chapter 4: Results

This chapter shows in detail the main results of the study, which is to identify the amount of power that each node in the test network can incorporate without causing overloads to the system elements. The impact of the variable capacities of the transmission lines is detailed in terms of the existence of overloading in the contemplated scenarios, not only in the power that a node can accommodate.

The effect of tolerance regarding the number of hours in which it is allowed to identify overloading when additional power is injected into a node of the transmission network is summarized in this chapter.

The possibility of using this tool to identify elements of the transmission network that are prone to becoming bottlenecks due to generation additions in a particular node is mentioned. Furthermore, the impact of variable capacities on the timing of overloads in the system is also detailed.

1.3.5 Chapter 5: Conclusions

This section summarizes the main findings of the study and its final scope based on the premises and considerations described. It also describes the secondary results obtained from the implementation of the designed methodology.

This complementary section includes possible practical uses for a tool of this type in a medium and long-term planning context, both for the generation matrix and for possible transmission projects to be incorporated into the system, as a result of optimal criteria for investments.

2 Literature review

The transport capacity of the transmission lines in a power system plays a crucial role in maintaining energy stability and efficiency. As energy demands continue to rise and renewable sources become more integrated, research into evaluating and optimizing transmission capacity has become increasingly important. The literature review explores the transmission capacity of transmission lines from various perspectives while analyzing the effects of environmental conditions. This analysis aids in determining static, seasonal, and even hourly limits for transmission capacity evaluation. Moreover, the study investigates essential criteria for power transmission systems planning. These criteria enable optimal resource utilization and appropriate response to future demands.

This analysis considers the adequacy of transmission capacity and operational security of transmission systems to determine the impact of transmission constraints on potential sites for new power plants, in order to minimize the need for extra network investments to integrate this generation in the medium- and long-term planning.

2.1 Carrying capacity for transmission lines

To determine the current that an overhead conductor can safely carry, it is necessary to analyze the heat transfer of the conductor to the environment. As a consequence of the Joule effect, conductors increase their temperature when carrying electric current in them. It is necessary that the temperature of these conductors is kept within the limits established for each type of alloy and combination of materials used in their construction, in [1] and [2] the most common and accepted standards for the calculation of ampacity in overhead conductors are compared.

2.1.1 Heat transfer in overhead conductors

Both [3] and [4] describe methodologies for calculating the ampacity of overhead conductors in a steady state based on the thermal equilibrium between the heat absorbed by the conductor and the heat transfer mechanisms with the environment that performs cooling functions. Equations 1 and 2 show the relationships used by IEEE and CIGRE respectively.

$$P_J + P_S = P_C + P_r \quad (1)$$

$$P_J + P_M + P_S + P_i = P_C + P_r + Pw \quad (2)$$

The terms on the left-hand side represent the heat absorbed by the conductor, while on the right-hand side of both equations is the heat dissipated by the conductors, specifically:

- P_J Joule effect heating
- P_M Magnetic heating
- P_S Heating by solar radiation
- P_i Heating by corona effect
- P_C Convection cooling
- P_r Thermal radiation cooling
- P_w Evaporative cooling

Under steady-state operation, it is required to calculate as best as possible the amount of heat from each source mentioned above. Each term will depend on different environmental and operational variables such as ambient temperature, solar radiation at the site, current in the conductor, and material resistance, among others.

2.1.2 Joule effect heating

The most relevant term for ampacity calculations is the Joule effect term since it depends on the two most relevant parameters for the operation of an electrical power system. $P_J = P_J(I, T_{avg})$. The heat absorbed under the Joule effect is calculated as follows [3].

$$P_J = k_j I^2 R_{dc}\left[1 + \alpha\left(T_{avg} - 20\right)\right] \quad (3)$$

Where:

- k_j Is the adjustment factor for the resistance in AC due to skin effect and magnetization in AC operation. It is equivalent to 1.0123
- I Is the RMS current on the conductor
- R_{dc} Is the DC resistance per unit-length in Ω/km
- α Is the temperature coefficient to account for changes in resistivity of the conductor, in K^{-1}
- T_{avg} Is the average temperature of the conductor.

2.1.3 Magnetization heating

AC magnetization impacts the heat produced in the conductors due to the effect of Eddy currents, and the ferromagnetic behavior of the materials in the core of the conductors used in transmission and distribution. From experimental results, an empirical relationship for the heat absorbed by magnetization at 50 Hz has been determined. [2] [5].

$$P_M = 4.90 \times 10^6 d^{1/2} A B_m^{1.82} \, exp(-2.5 \times 10^{-3} T_{core}) \quad (4)$$

The terms are:

- d is the diameter of the conductor
- A is the cross-sectional area of the conductor
- B_m is the magnetic induction on the ferromagnetic material
- T_{core} is the average temperature on the core of the conductor.

2.1.4 Solar radiation heating

This factor depends greatly on the atmospheric conditions and the site's geography where the conductors are located. Furthermore, a conductor heat-absorbing capacity hinges upon its diameter, relative inclination to the horizontal axis, and material absorption capacity. The heat absorbed from solar radiation per unit length can be calculated as a simplified version of the method introduced by the CIGRE standard. The calculation considers the global radiation on the conductor [3].

$$P_S = \alpha_s S D \quad (5)$$

The terms are:

- α_S is the absorption capacity of the material, it ranges from 0.23 to 0.95, for practical and general applications it is possible to use 0.5
- S is the solar global radiation
- D is the diameter of the conductor

More intricate techniques based on separating direct and diffuse radiation and making site-specific solar radiation estimates exist. Nonetheless, with the possibility of measuring solar radiation at the surface level and the readily available information, the simplified method carries advantages in implementing it.

2.1.5 Convection cooling

The first mechanism by which the conductor dissipates heat to reach a state of thermal equilibrium is convection. This type of cooling relies, among other factors, on the velocity and angle at which the wind hits the conductor. This dependence will be indicated in the corresponding term of the equations described in [2] and [3].

$$P_C = \pi\lambda_f(T_s - T_a)Nu \quad (6)$$

From equation 6:

- λ_f is the thermal conductivity of the air
- T_s is the Surface temperature on the conductor
- T_a is the ambient temperature on site
- Nu represents the Nusselt number, a constant that considers the wind effect on the convection cooling.

The Nusselt number is determined by the Reynolds number, an adaptable coefficient dependent on the wind speed, medium viscosity, and air density. Empirical relationships can be applied to estimate the Nusselt number for different wind conditions, but a detailed fluid mechanics discussion is beyond the scope of this work.

The IEEE-738 standard provides a simpler method for determining heat dissipation caused by thermal convection. Equations 7 and 8 differentiate between low and high wind speeds, describing the amount of heat released by convection in each case [4].

$$P_C = K_{angle}\left[1.01 + 0.371\left(\frac{D\rho_f V_w}{\mu_f}\right)^{0.52}\right]k_f(T_c - T_a) \quad (7)$$

$$P_C = K_{angle}\left[0.1695\left(\frac{D\rho_f V_w}{\mu_f}\right)^{0.60}\right]k_f(T_c - T_a) \quad (8)$$

In which

- D represents the diameter of the conductor
- ρ_f is the density of air
- V_w is the wind velocity
- μ_f represents the air velocity

- k_f is the thermal conductivity of the air
- T_a is the ambient temperature on site
- T_c is the conductor temperature
- K_{angle} is a correction factor that accounts for the angle at which the wind strikes the conductor. It is calculated from the angle ϕ between the conductor and the incident wind speed. For general application an angle of $\phi = 45°$ is used.

$$K_{angle} = 1.194 - cos\,\phi + 0.194\,cos\,2\phi + 0.368\,sin\,2\phi \quad (9)$$

2.1.6 Thermal radiation cooling

Both IEEE and CIGRE standards provide simplified, and equivalent, relationships for heat emission by thermal radiation. In [3] the heat loss by this mechanism is described by the following equation.

$$P_r = \pi D \epsilon \sigma_B [(T_s + 273)^4 - (T_a + 273)^4] \quad (10)$$

In which

- D represents the diameter of the conductor
- ϵ is the emissivity factor of the surface of the conductor, it typically ranges from 0.23 to 0.95. It is common, for general estimations, to use 0.5
- σ_B is the Stefan-Boltzmann constant
- T_s is the temperature at the surface of the conductor
- T_a is the ambient temperature

2.1.7 Additional terms

Both IEEE and CIGRE standards omit terms related to corona heating and evaporative cooling from the calculations. The former is omitted because it is negligible unless there are high voltage gradients, which exist under special conditions and are not predominant during average operation. The evaporative cooling term is omitted because it depends on whether the conductor is wet, as in the case of rain in the area, but does not vary significantly with changes in relative humidity [3]. These terms can be included in dynamic estimates during real-time operation, but for design purposes they do not represent typical environmental conditions during operation.

2.2 Transport capacity estimations for overhead bare conductors

From equation 1 or 2 it is possible to establish an equation to calculate the amount of current that a conductor can safely carry in steady state. Combining either of the above equations with equation 3 gives the following relationship:

$$I_{rms} = \sqrt{\frac{P_C + P_r - P_M - P_S}{k_j R_{dc}\left[1 + \alpha\left(T_{avg} - 20\right)\right]}} \qquad 11$$

The IEEE standard omits the P_M term for heating due to magnetization of the conductor core. For calculation purposes using Equation 11, the term T_{avg} would be the maximum temperature the conductor can reach in steady state without compromising its mechanical integrity while maintaining the required clearance to ground [4]. In equation 11, k_j is the adjustment factor for the resistance in AC due to skin effect and magnetization in AC operation. α represents the temperature coefficient for the resistivity of the conductor [3].

2.2.1 Effect of the ambient temperature

Equations 6-8 and 10 demonstrate the effect of ambient temperature on conductor heat dissipation and the expected variation in ampacity based on prevailing environmental conditions. Reference [6] shows the impact of ambient temperature on the conductor's temperature while carrying a fixed amount of current. Reference [7] takes a similar approach and presents the effect of different parameters on conductor ampacity under IEEE and CIGRE standards criteria. In [8], the text illustrates the impact of each cooling type in thermal equilibrium on the conductor ampacity.

The approximate effect of ambient temperature on heat dissipation is demonstrated by utilizing equations 6 and 10 to establish a ratio of heat dissipation per unit relative to the base case of 40°C. The impact of heat dissipation on the ampacity of the conductor is not direct, but it is still significant. At temperatures below 20°C, this effect is particularly noticeable. This would impact in a more significant manner at locations in which the average temperature ranges widely.

Figure 1: Effect of ambient temperature on heat dissipation

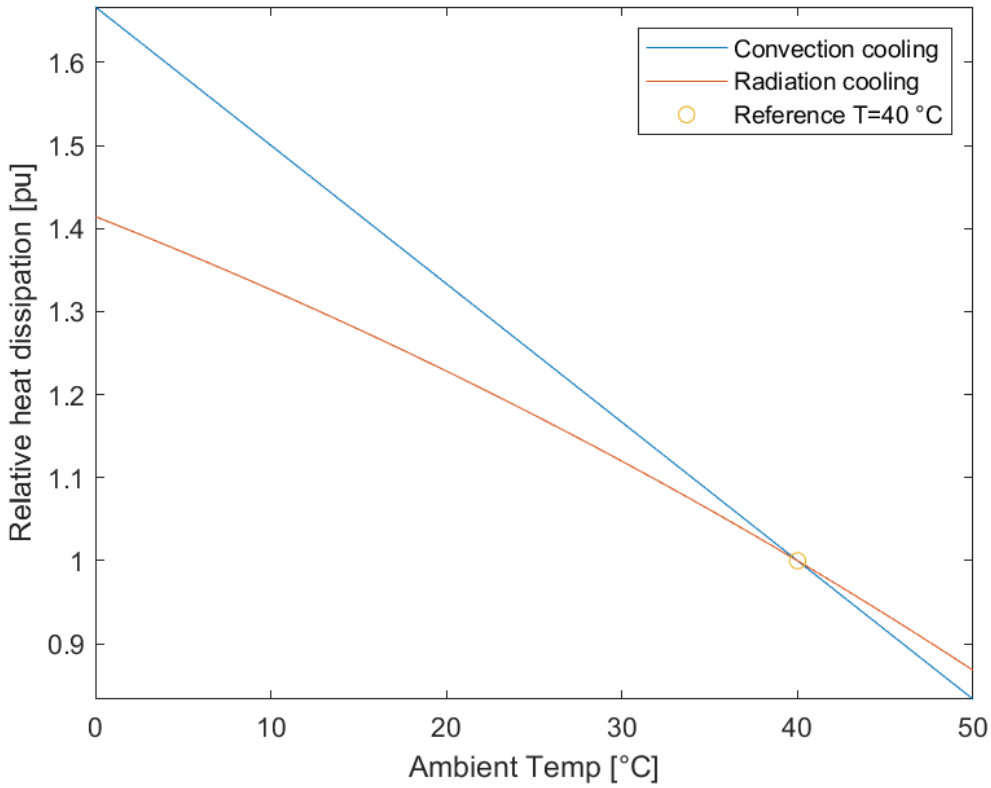

Source: Made by the author

As climate conditions shift, it will be imperative to factor in fluctuations in ampacity resulting from lower winter temperatures or higher summer temperatures. Reference [9] provides an assessment of the long-term influence on transmission line ampacity, with a projected decrease of 2% to 8% in transmission capacity by 2080 based on various greenhouse gas concentration scenarios.

The figures display how the ambient temperature affects the conductor's ampacity or the temperature it reaches at a constant current. This highlights the significance of precise ambient conditions when estimating the carrying capacity of overhead transmission lines.

Figure 2: Ambient temperature effect on ampacity [7]

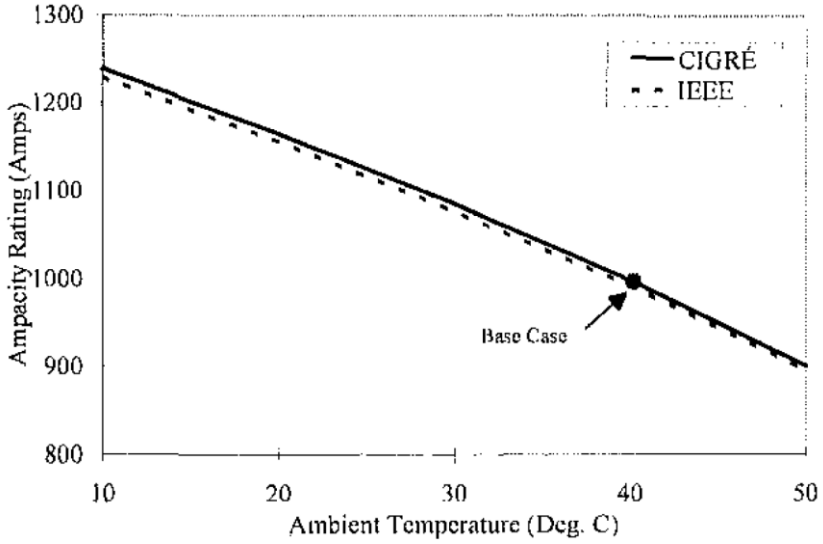

Figure 3: Ambient temperature effect on conductor temperature [6]

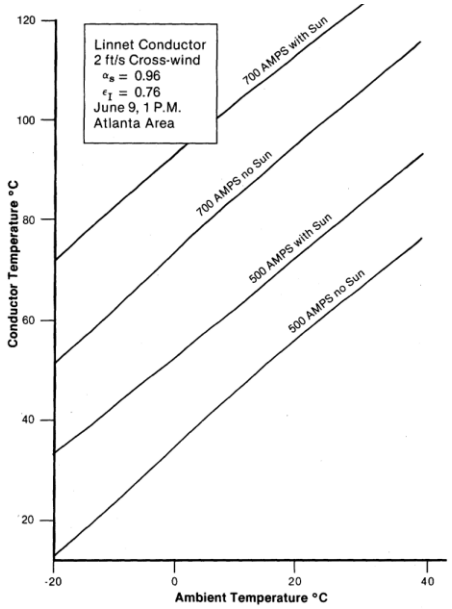

2.2.2 Effect of the wind speed

Equations 7 and 8 incorporate the effect of wind speed on conductors into the calculation of convective heat loss. These equations describe the effect of speed as a magnitude and the direction in which the wind is incident on the conductor. It is expected that the cooling effect of air currents will be greater with perpendicular incidence than with parallel incidence. It is also expected that a higher wind speed will have a more noticeable effect on the conductor temperature.

In [10], the effect of wind speed and direction on the cooling and temperature of a conductor is described, which, as described in Section 2.1.5, affects the amount of current that the conductor can safely carry in steady state. It is clear that heat dissipation gains are not linearly related to the ampacity of the conductors, but there are improvements to be made by using more detailed wind

speed information in the operating zone of the lines. The effect of wind speed has been analyzed in detail in [11].

Figure 4: Wind speed effect on convection cooling

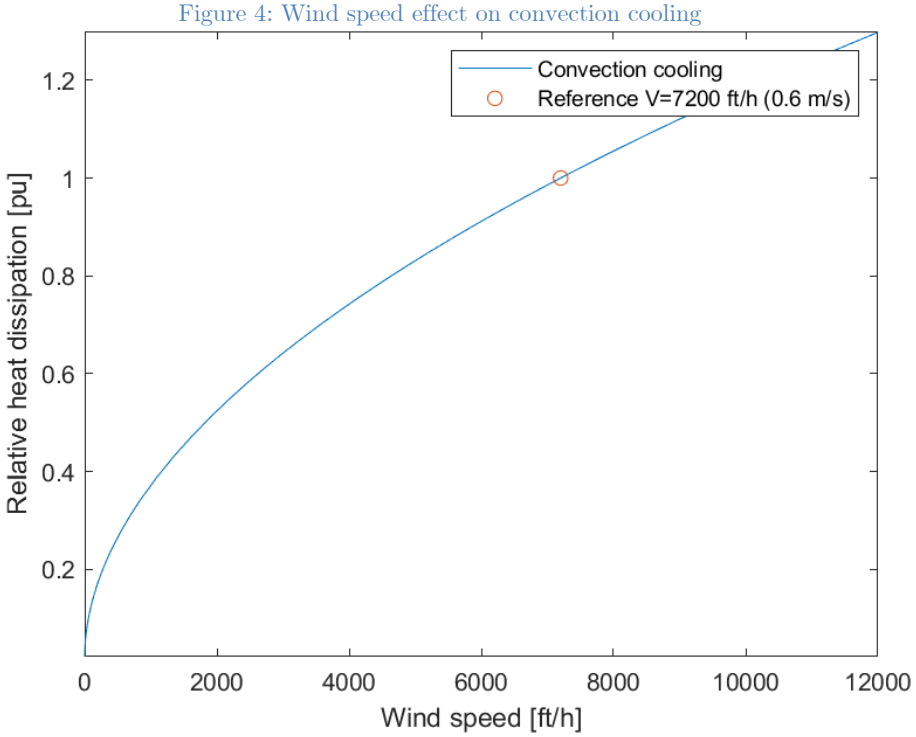

Source: Made by the author

Figure 5: Wind angle effect on convection cooling

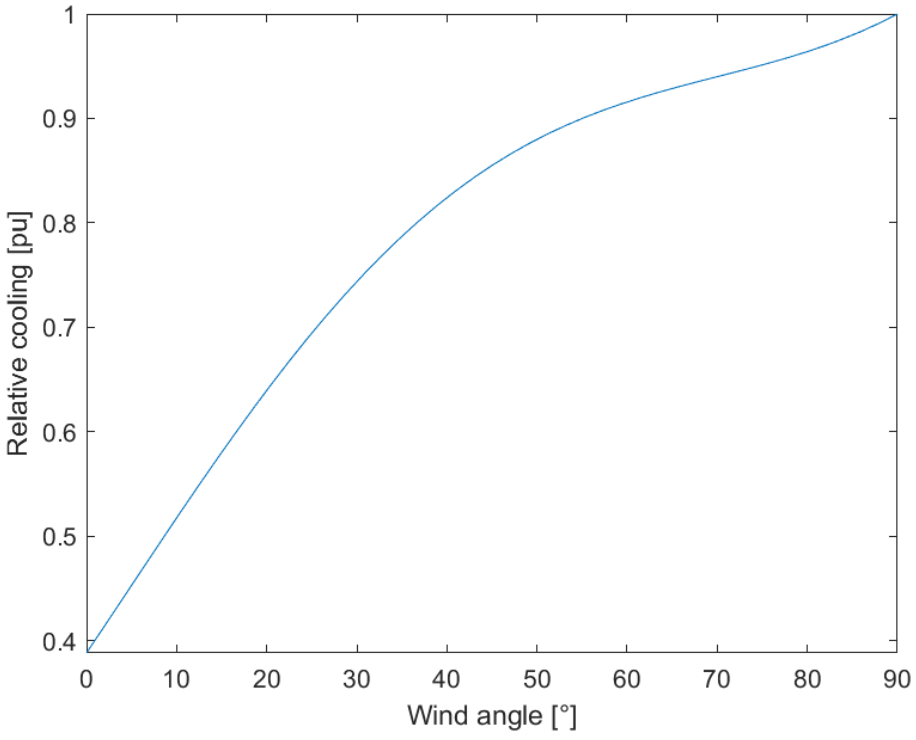

Source: Made by the author

Wind speed is typically utilized in dynamic estimates of carrying capacity, but it's also feasible to incorporate statistics of this variable to account for the

anticipated effect on the ampacity of an aerial conductor. This enables better accuracy in carrying capacity estimates for situations that do not require real-time estimates, like those that are required in this analysis. In studies like those featured in [12], wind speed patterns are illustrated with hourly and seasonal resolution statistics. This serves to enhance the precision of calculating conductor ampacity.

2.3 Criteria for transport capacity estimations used in system operation

2.3.1 Static Line Rating - SLR

The typical approach is to employ a static calculation under unfavorable environmental conditions, often utilizing low wind speeds alongside high solar radiation and elevated ambient temperatures. Temperatures above 35°C and solar radiation nearing $1000\,W/m^2$ are commonly taken into account [13]

Using this method, a conservative estimation is obtained, generally resulting in an underestimated amount of current the conductor can carry during normal operation. Using environmental conditions closer to reality is expected to enhance the conductor's heat dissipation capability. The static approach is frequently employed as it simplifies the computation of conductors' carrying capacity and provides a substantial safety margin for system operators. Typically, there is a long-term static limit for normal operational conditions, and a higher emergency limit used in the event of contingencies or power system disruptions [14].

2.3.2 Seasonally adjusted rating - SAR

One way to enhance the static capacity model is by incorporating seasonal adjustments to the transmission line carrying capacity. This is particularly applicable in areas where distinct seasons exist, with significant fluctuations in ambient temperature and solar radiation throughout the day. Such conditions are common in high latitudes of both the northern and southern hemispheres. Although [13] briefly discusses the significance of seasonal adjustments based on the available climate model, more extensive research is necessary.

In [15], it is recommended that regions with ambient temperature differences of approximately 10°C between seasons establish seasonal transport capacities for normal and emergency operations to optimize transmission infrastructure in colder months.

As for seasonal adjustments, [16] advises their use for long-term planning purposes. It is noted that operators define seasons, which should consist of at least

four seasons per year. The seasons should reflect realistic ambient temperature conditions to provide operators with flexibility in defining the seasons based on each zone of influence.

2.3.3 Ambient adjusted rating – AAR

The next phase in enhancing the model is to implement temperature-specific adjustments in greater detail. Broadly speaking, there are two methods: one utilizes seasonal adjustments, while the other takes a more in-depth, continuous approach. The next phase in enhancing the model is to implement temperature-specific adjustments in greater detail. It should be noted that dynamic adjustments based on real-time measurements will not be explored at this time. This topic has been thoroughly researched by numerous professionals and scholars, and detailed results can be found in [17].

In the review of [15], it is noted that the initial description for these detailed adjustments has been mentioned along with suitable precautions during their implementation. These precautions are particularly sensitive to the wind speed being considered. The report also states that when using the AAR in nighttime conditions, the variable that is usually altered is solar radiation, while common considerations include only variations in ambient temperature, with other variables held constant.

FERC Order 881 [16] states the implementation of AAR is necessary before DLR can be initiated. The directive specifies that AAR should only be considered for up to an hour and estimates should be based on the average temperature in the transmission line's area of influence.

Consequently, implementing AAR or SAR is expected to enhance the transmission network's carrying capacity. This is crucial for transmission lines with network congestion. In [18], AAR's effects on dispatch and operation efficiency in the electricity market are further explained by reducing or eliminating transmission network congestion to meet demand.

2.4 Considerations used in transmission expansion planning

Long-term planning requires an evaluation and anticipation of the future requirements of the transmission grid to ensure readiness for demand growth, new technology integration, and infrastructure changes.

Identifying the node's capacity to safely handle additional power can establish suitable locations for new generation plants seeking participation in the electric system. Due to limitations in the construction of new transmission lines, it is

necessary to identify the optimal location that requires minimal investment to the transmission infrastructure [19] [20].

Access to the transmission network and possible transport restrictions due to this type of infrastructure are essential criteria in selecting suitable locations for new power plant installations. One of the primary goals of expanding generation and transmission is to minimize investment costs in generation facilities as well as transmission infrastructure [21].

Site optimization for a new power plant affects different infrastructures required for its operation in varying ways. One example is the presence of roads, the accessibility of water and telecommunications services, and most importantly, access to the transmission network. This is because the absence of these elements escalates the investment costs of the power plant, thereby reducing its feasibility for long-term development. In [21], a methodology is established to weigh the factors associated with the location of the power plant. However, in this work, a similar methodology will not be considered. Instead, the goal is to identify those nodes within the transmission network that allow for the highest power injections without the need for additional investments in the grid.

One of the algorithms utilized for planning transmission expansion is the investment optimization problem. This problem involves using discrete decision variables [22]. It is typical for centralized planning to weigh significant generation projects that can meet energy demands over the lifetime of the projects. Although smaller-scale distributed generation is gaining momentum, large-scale generation plants remain relevant and complement distributed generation in safe and reliable power system operation [23].

Large-scale generation plants offer significant benefits, including improved efficiency and financial advantages associated with their greater capacity. A compilation of trends in thermal efficiency by capacity, as presented in [24], shows that simple cycle natural gas units and internal combustion engines experience the most significant impacts. Other factors, such as the installation and operation costs of a power plant and its levelized cost of energy, have been extensively investigated from an economic standpoint [25] [26].

This is a secondary context for the objectives of this work, however, it is important to show the relevance of the size of the generation plants that will participate in an electricity market, since this will have a long-term impact on the total costs of the operation of a system. Various operators in different regions refer to the identification of the transmission capacity of the transmission network

for short- and long-term planning studies. The NE-ISO documentation was utilized as a reference for this task since their area of influence is in the northeast United States [27] [28] [29] [30].

2.5 Operational security and sufficiency in power systems

2.5.1 Power systems reliability

Reliability is vital in ensuring a system operates continuously, providing uninterrupted service to meet demand. It is a relevant consideration in the planning, operation, and maintenance of electrical power systems, as it aims to guarantee that end-users have constant access to electricity, with minimal or no significant power outages [31].

Users in an electrical system, whether consumers or producers, expect the system to be able to withstand unforeseen and random events. Therefore, it becomes essential during the planning phase to consider the required long-term and medium-term investments to meet reliability and capacity restrictions. This must be done without compromising the economic aspect of the system operation [32].

An electrical system must withstand diverse conditions since the operating state is constantly changing. The factors that affect the variability of an electrical system are unpredictable. These factors could involve alterations in user demand, primary resource availability, and environmental conditions, among others. It is also important to consider the transition from a system with complete availability to one that is prone to forced unavailability or failures [33].

2.5.2 Probability in the context of electrical power systems

An initial and deterministic method for estimating the reliability of an element or system is by utilizing a probabilistic approach that counts the frequency of recorded undesired conditions within the system. If historical data is available, it can be used to estimate the reliability indicator by applying the applicable relationship.

$$P_{occurrance} = \frac{N_{occurrance}}{N_{total}} \qquad 12$$

Where $P_{occurrance}$ represents the likelihood of the event happening, $N_{occurrance}$ is the number of recorded scenarios where the event has occurred, and N_{total} is the total number of scenarios analyzed [31]. Evaluating historical information is an important first step in determining the possibility of an event occurring in the

electrical system. For instance, assessing the probability of failure in an element during its operation time.

In some cases, historical data may not suffice to anticipate the likelihood of an event, particularly when it is dependent on the occurrence of a prior random occurrence. For instance, determining the likelihood of a transmission line overloading because of a contingency of another transmission line under certain operating conditions. In situations like the one described, it is common to apply the Bayesian statistical theory to conditional probability [31] [34].

One feasible option for a probabilistic approach is to analyze different operational scenarios of the electrical system, whether real or simulated, and consider variable factors such as power demand, generation availability, transmission capacity, and other pertinent parameters. For each scenario, a series of outcomes is generated, which may provide data on the frequency of undesired conditions like failures or overloads. Utilizing this data, equation 12 can be applied to estimate the likelihood of the event of interest, in this instance, an overload resulting from a single contingency.

After sufficient scenarios have been considered, it is decided if the probability of occurrence falls within the tolerances set by the relevant regulation or accepted practices in the context. For instance, [35] states that for elements operating at 138 and 69 kV, each element is allowed a maximum of 3 forced unavailability events per year, with a total duration of 300 minutes or 5 hours. This equates to less than 1% forced unavailability per year.

NERC also defines similar indicators, focusing on the duration of unexpected disconnections, cumulative time of momentary, and sustained disconnections [36]. Previous studies have examined the availability of transmission network elements, including transmission lines and power transformers, in US systems. From 2018 to 2022, transmission lines had an average unavailability of 0.254%, while power transformers had an unavailability of 0.22% [37]. This marks a difference from previous reports and suggests a noticeable enhancement in network element availability indicators. However, in the 2012 report version, the indicator takes into account planned disconnections [38]. Therefore, to make an accurate comparison, appropriate categorization is required.

Section 3.1 summarizes a procedure based on these concepts to calculate the likelihood of overloads in the transmission system, then factoring in added generation in a network node, and a single N-1 contingency. This is to determine if there are more scenarios in which it is possible to allocate more generation in a

node, given than the tolerance established in the methodology allows for this new power. It is a method of extrapolating the availability concept to identify the probability of network overload under adverse system conditions, in accordance with the sufficiency criteria of power systems.

2.5.3 Sufficiency of electrical power systems

Sufficiency refers to the ability of an electrical transmission network to meet electrical demand while maintaining the safety limits of the equipment and infrastructure in the region, considering changes in user behaviour or energy production patterns. In simpler terms, it is the transmission system's ability to transport the required amount of energy to the consumers without any congestion or instability risks [39].

In general, ensuring the sufficiency and safety of an electrical system requires careful consideration of various aspects. Factors to consider include current and future demand, unit availability for generation, transmission network topology and infrastructure status, and the involvement of various types of power plants in the generation matrix.

NERC Standard 51 defines, in the context of operational security, the events that lead to a single N-1 contingency. These events include single-phase or three-phase ground fault that disconnects a generator, transmission line, or power transformer. Emergency thermal limits apply to the elements and conductors under such conditions. Additionally, the system must remain stable without presenting load losses or cascade disconnections [40].

In the prior section, it was mentioned that the likelihood of overloading an element was dependent on the incidence of an N-1 contingency within the network. However, the sufficiency criteria indicate that the system must withstand the most adverse operating conditions. While it's not feasible to prepare for every possible event, it's required to prepare the system to endure extreme conditions that have a high impact on it.

The focus of this work is on the transmission network, to prevent it from being a bottleneck that affects the economically efficient operation of the entire system. Identifying the maximum power capacity of the network is crucial to ensure sufficient and reliable supply, thereby preventing non-compliance with the security criteria specified in relevant regulations. Ensuring the sufficiency of the power system is crucial in identifying both expansions in the transmission network and additions to the generation system. Considering potential transportation

limitations becomes crucial in specifying the primary investments in the system that yield greater positive outcomes.

2.5.4 Criterion for operational security

Operational safety criteria are rules and limits established to ensure the stability, reliability and safety of the electrical transmission system during operation. These criteria are essential to avoid overloads, instability and failures that could affect the power supply and the integrity of the equipment. Among other aspects, the thermal capacity of the transmission lines, power bars and transformers, permitted voltage ranges, reactive power control, sufficient regulation reserves for the generation matrix and correct operation are considered for the operational safety of the system. of protective equipment [20] [39].

In this work, particular emphasis is placed on the thermal capacity of conductors, and how environmental conditions affect their ability to transport energy, described in sections 2.2.1 and 2.2.2.

A common description of the thermal capacity of a conductor is the maximum limit of current that can flow continuously through a transmission line without exceeding its heat dissipation capacity. Keeping currents within the thermal capacity ensures that the lines do not overheat and deteriorate rapidly. The conductors can temporarily withstand an amount of current greater than their thermal capacity. In [41] it is indicated as an example that a conductor can withstand 115% of its continuous thermal capacity for a period of 15 minutes. The specific value is determined by each operator or regulator. In this work, the limits are specified in section 3.6, using the regulation in Honduras as a reference [42].

3 Methodology

Previously it was mentioned that the purpose of the work is to build a mechanism that allows the estimation of the power injection limit, or hosting capacity, of the nodes in a transmission grid. A way to achieve it is to set a tolerance of hours during which it is acceptable to order the plants to reduce their output due to technical restrictions in the grid. It is expected that the restrictions represent less than 1% or 2% of the hours in a year, although this criterion can differ based on local regulations and practices.

The restrictions are given to prevent overloading on the grid, both in normal operating conditions and operation after a contingency. It becomes necessary to identify the number of hours in which overloading conditions are expected within a typical operational day. On these premises it is possible to simulate the power flows on the grid on N-0 and N-1 operational conditions for all of the hours in the year, considering the expected demand and expected dispatch of the power plants in the system. The expected conditions can be extrapolated from historical data, or extracted from optimization tools used for short and long-term planning.

The difficulty that arises from this approach is the computational effort and simulation time required to consider all required combinations. For any particular year there are 8760 hours, a k number of nodes, j contingencies to consider, and monitor the power flow for i transmission lines. All of that is added to a discrete set of power injections, $P_1 - P_N$,that are considered additions to each node. An alternative approach is to sample the year and build a set of hours, or operational scenarios, that capture enough details of the typical conditions for the system through the year. Typically, a deterministic approach is used, in which only the most extreme cases for a season are considered. It is common to use the scenarios with the highest and lowest load of the season, however, this approach fails in capturing the details of the operation within the hours between these high-demand moments.

The sampling considered within the scope of this work considers 288 operational scenarios, a 24-hour set, or a typical day, for each month of the year. The typical day is built considering the average load and generation profiles for each month. This approach allows to capture the information regarding the peak and minimum load, and the hourly variations between them. Also, the approach includes information on the monthly variations that reflect the load patterns and the differences within the available generation resources during the year. The specific procedure to assemble the 288 scenarios will be discussed in subsequent

sections, this method and procedure can be modified to fulfill the different needs of a specific system or restrictions.

Sampling makes it possible to reduce execution times and find the number of hours h, in which overloading occur in the transmission grid due to the injections by a new power plant with capacity P_n into a node n. The power will be admissible for the grid if the number of hours meets the condition $h < h_{tol}$, where h_{tol} represents the maximum number of hours in which power curtailments are allowed to mitigate possible overloads. If the condition is met, it is possible to increase the power P_n within the established range $P_1 - P_N$, and in this way verify if the node can accommodate a higher power without additional reinforcements to the transmission network.

In addition to this, the effect of using transmission line capacity adjustments based on seasonal and even hourly environmental conditions is included. The criteria used are the seasonal adjustment rating (SAR), and the hourly ambient adjustment rating (AAR). Dynamic line rating (DLR) is not included, as it serves a different function than the purpose of this analysis. DLR fulfills an operational function in real-time, as it monitors the meteorological variables during the operation and allows faster adjustments to the available capacity in hourly or intra-hourly dispatch.

Combining these factors and considerations, the admissible power P_n will be identified, which is acceptable under the established tolerances and operational safety criteria. The impact of the adjustments on the capacity rating will also be compared to verify if there is a significant benefit in the amount of power that a node can accommodate. This is a decision criterion for the incorporation of plants into the generation park, so that the safety and reliability of the system are not compromised, and that the operation does not incur cost overruns due to compensation for generation curtailments, or dispatch of units with higher variable costs due to apparent transmission restrictions.

The detailed sequence of steps to obtain these results, and additional results, will be described in later sections of this chapter. Arguments about the scalability and adaptability of this methodology or logical sequence to satisfy different operational, statistical or regulatory criteria will also be presented.

3.1 Summary

As a starting point, real information is available on the operation of the Portuguese electrical system for the year 2021. Based on this information, operating scenarios were built, these scenarios capture the relevant operating

conditions, as well as possible variations in demand and generation technologies used to meet said demand.

After the initial processing of the information, the resulting data was adapted so that it can be incorporated into the available transmission network model. This is to be able to execute power flows that allows validating the operation without power additions, both in N-0 and N-1 conditions. For this analysis, the N-2 criterion was not considered due to the exponential number of possible contingency combinations, which would increase the computational effort and necessary simulation time. However, it is possible to incorporate this criterion into the analysis if required by the corresponding technical premises.

The next step is to perform power injections from P_1 to P_N for all the nodes of the transmission network individually. Initially, power flow simulations are carried out on N-0 conditions, and the loading of the transmission lines is monitored with all the elements in service. This is to identify if the additions cause overloads that force curtailments, or that directly make it impossible to operate in that particular node. From this step, h_{N-0} are obtained in which overloads are recorded as a consequence of the addition of power in a node n of the system. Ideally, the value h_{N-0} is zero, however, it is expected that for large power additions, some scenarios could register overloading.

The procedure continues by simulating N-1 contingencies considering the additional injections into the nodes. Once again, the loading of the transmission lines in service is monitored, to quantify the number of scenarios in which overloads occur as a result of the power additions P_n. The number of hours, or operating scenarios, under which overloads are recorded in this step is called h_{N-1}. This value is expected to be greater than zero, and greater than h_{N-0}, identified in the previous step.

These steps are repeated for all power values P_n within the range $P_1 - P_N$, and all selected nodes. From this, for each node n and each power P_n, a value h_{nP} is obtained, which is the sum of the counted scenarios under N-0 and N-1 conditions. The total value is represented in the form $h_{nP} = h_{nP_{N-0}} + h_{nP_{N-1}}$. To identify the maximum value of power P_n, h_{nP} is compared with the tolerance h_{tol}, and the maximum power that a node n can allocate is reported.

This procedure can be performed for different ratings in the transmission lines. Three ratings were used for this study, a static line rating (SLR), seasonal adjustments in the rating (SAR), and hourly adjustments for ambient conditions (AAR).

The final result of this process is a power value P_n that can be accommodated in a transmission node for each type of rating adjustment. In summary $P_{n_{SLR}}$, $P_{n_{SAR}}$, and $P_{n_{AAR}}$ are obtained. This serves to contrast the effect of the adjustments made to the carrying capacity of the elements of the grid and allows for the optimal operation of the system.

3.2 Load and generation profiles

To build the representative scenarios, the annual information on the operation of the Portuguese electricity system for 2021 was used. With this information, a representative day was built for each month, where the hourly demand was the average of the hourly demands of said period. Regarding the generation, this is available by technology, for each one a procedure similar to that of the demand was carried out, where the hourly dispatch power is equal to the average hourly generation for each month.

By constructing a representative day for each month, a total of 288 hourly operating cases are obtained, which represent the typical operation of the system during the year. The advantage of using the average values is to smooth out the extreme variations that result from anomalous conditions where the system demand shows significant peaks that are not common during the year. In this analysis an average value was selected, however, it is possible to carry out this procedure by using a percentile value, or directly selecting random days as representative samples of the typical operation. This criterion is adaptable to particular needs and requirements.

Another key aspect to mention is that the methodology is not limited to 288 hours a year, the sampling can contemplate a greater number of hours or even 8760 hours in a year, with the penalty in computational effort that increases significantly along with the number of simulations to perform. This disadvantage can be mitigated by reducing the number of buses for which it is desired to identify the hosting capacity or the number of contingencies relevant to a specific area of the transmission network.

3.2.1 Load behaviour

In general, the demand has marked variations throughout the seasons. In the winter months, there is an increase in the peak demand at night around 8:00 pm. As spring progresses, the previously observed peak decreases and the maximum demand at daytime and nighttime are similar, with reductions in the off-peak hours. In summer this behavior persists, with the nighttime peak being slightly lower in July compared to the daytime peak demand. Another aspect to mention

is that the nighttime peak demand tends to shift as nightfall occurs later in the day. Finally, in the last three months of the year, the peak demand at night increases relative to daytime hours.

The behavior observed in the following figures shows the importance of seasonal variations in consumption patterns, which have a significant impact on system operation and therefore power flows in the grid.

Figure 6: Average load profile – winter

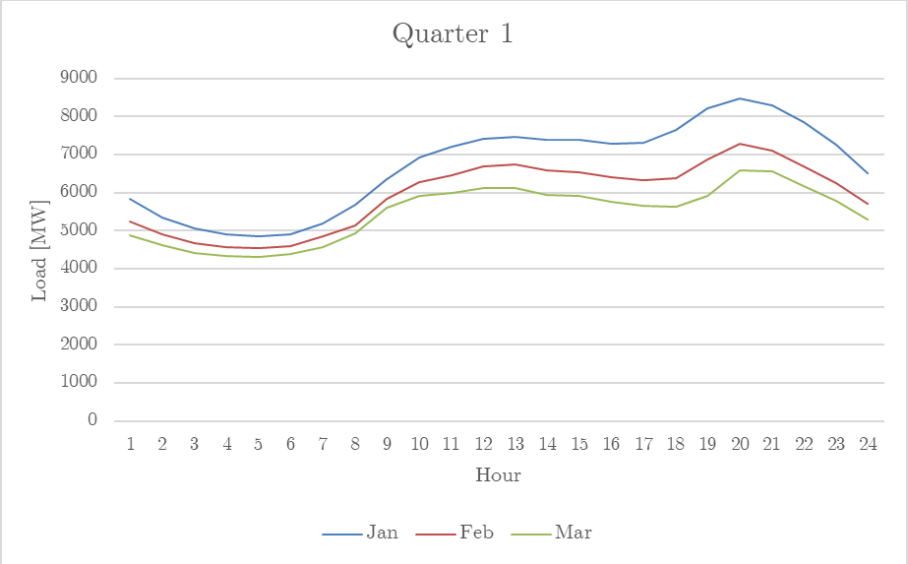

Figure 7: Average load profile – spring

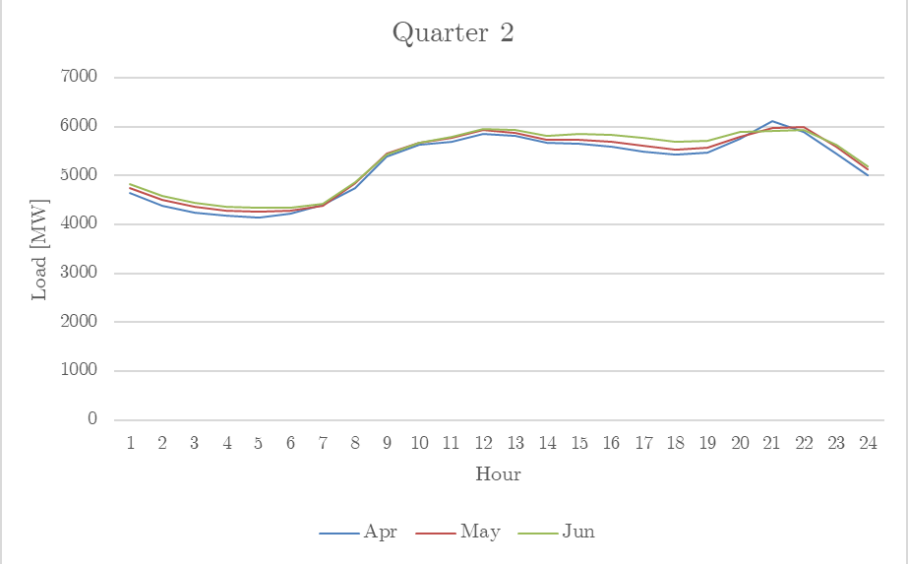

Figure 8: Average load profile – summer

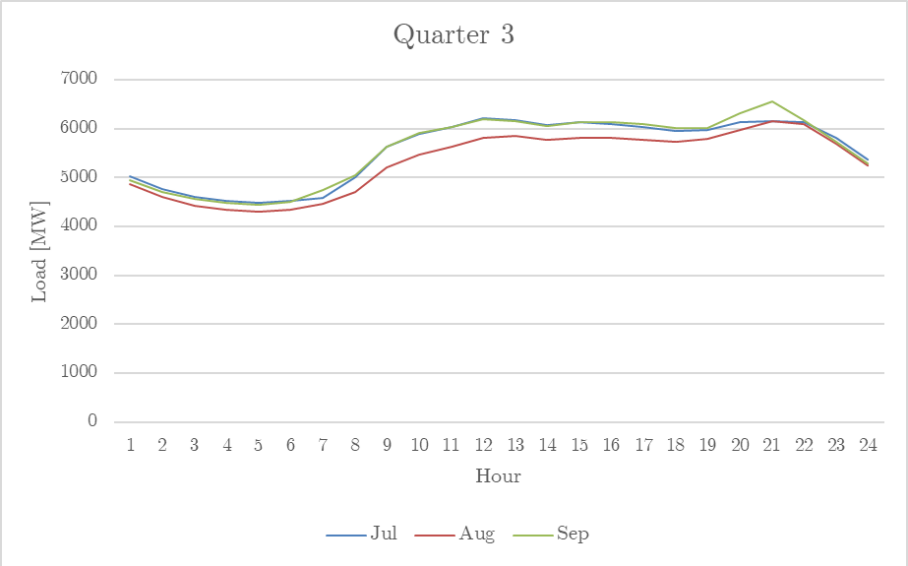

Figure 9: Average load profile – autumn

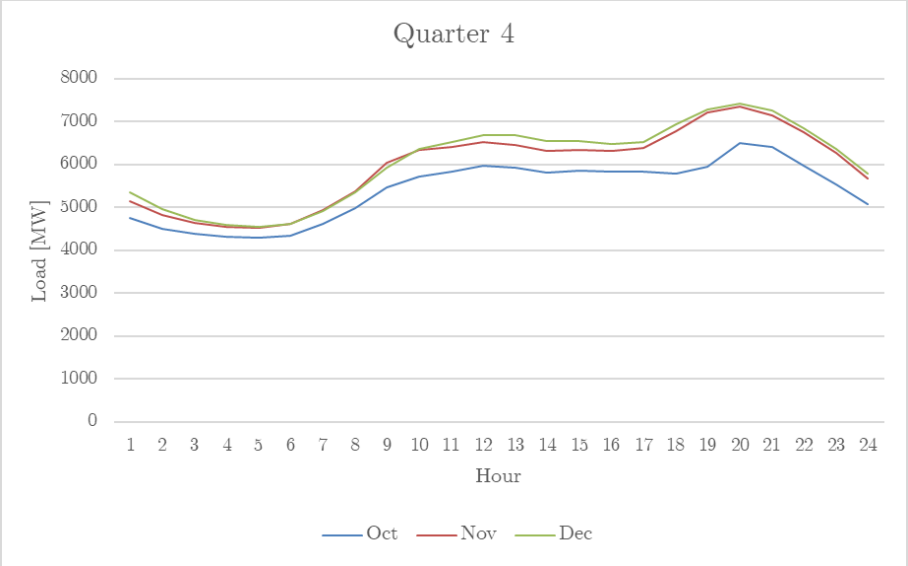

3.2.2 Generation

To simplify the behavior of the generation matrix, the information was condensed into four categories: solar, wind, hydroelectric and thermoelectric. The hydroelectric category included both dispatchable and non-dispatchable plants. Thermoelectric plants included natural gas, coal and bunker plants. Throughout the year the participation of these four categories changes based on the availability of solar radiation, wind, hydrological affluents and fuel costs. The representation of regional transactions with Spain was not included in detail, as this added a further layer of complexity, which is not necessary for testing the methodology. It is possible to adapt the information of the regional exchanges of a system to the model used, to consider this variable in more detailed analysis.

To show the impact of each technology, participation factors were calculated for each of the typical days considered. These will serve to scale generation in later stages so that its behavior corresponds to the demand values used in the transmission network model. At this stage, the average values in MW are not detailed, since these will be scaled, therefore, the unitary participation factors are more adequate to show the behavior of the technologies involved. These variations are more clearly illustrated from Figure 10 to Figure 21.

Once again, seasonal variations are noticeable. Regarding the participation of solar generation, it is reduced in the months of January, February and December, where the participation is close to 5% of the demand during the hours of maximum solar production. In the following months, it is observed that the solar curve increases in duration and height, reaching approximately 10% of the generation in the following months. The maximum solar production is reached in the months of July and August, where it is close to 20% of the demand during the hours of maximum solar production.

For wind energy production, is observed that it is predominant before dawn in the months of January, November and December, where it exceeds 40% of the hourly demand at that time, reaching more than 60% during the month of December. This is due to the high availability of wind and the lower demand at this time.

Thermoelectric power plants are mostly combined cycle units fueled by natural gas. In general, this technology shows stable behavior during the day and supplies around 30% of the hourly demand, except for the month of February, when its share fell to less than 20% of the total demand. This is associated with the high availability of hydroelectric power in this month.

The month with the greatest availability of hydroelectric generation is February, during which the share of this technology exceeded 50% of the system's demand. In the remaining months, a general pattern is observed, where hydroelectric production is significantly reduced during daylight hours. This is due to the available solar production and the common optimization criteria, where it is more appropriate to store water to produce electricity at times when demand increases and less, or no, variable renewable production is available. This pattern is observed in the figures, an increase in hydroelectric production at the beginning of the morning, followed by a drop in its production as solar production increases, and a subsequent increase at the beginning of the night to replace solar generation and cover the increase in demand, that is common at this hour.

Figure 10: Average generation profile – January

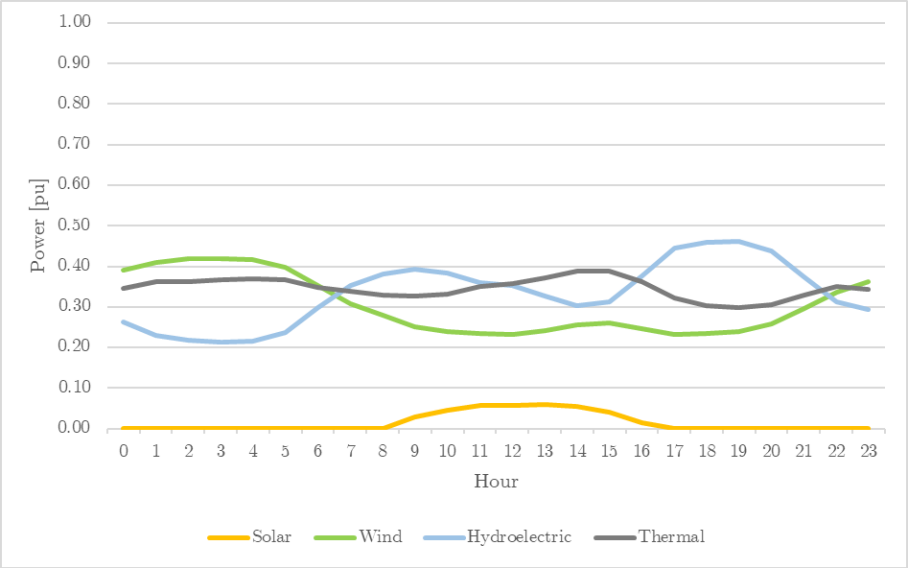

Figure 11: Average generation profile – February

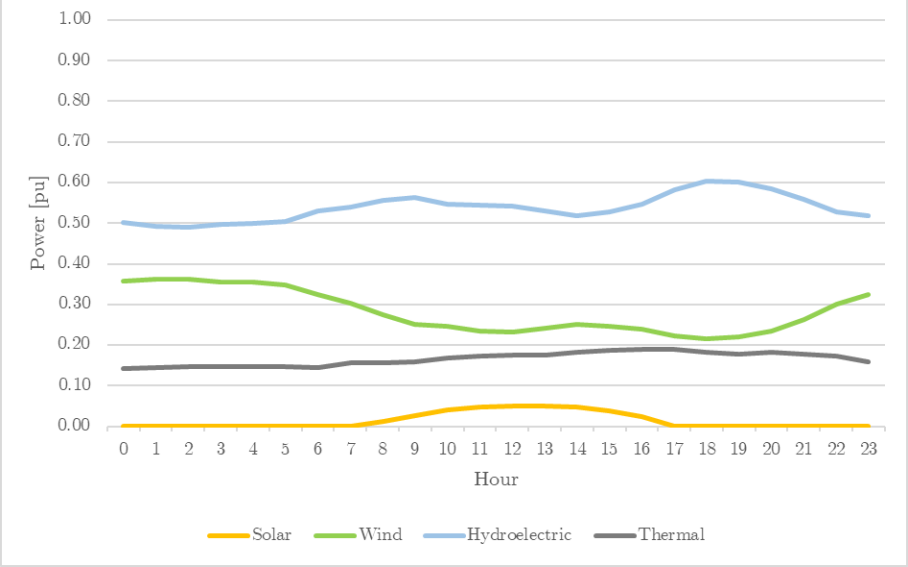

Figure 12: Average generation profile – March

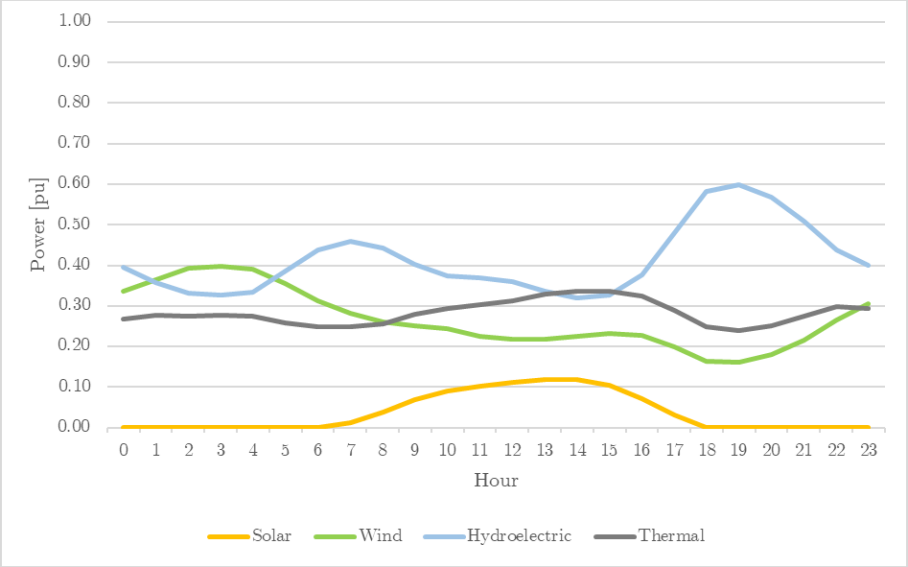

Figure 13: Average generation profile – April

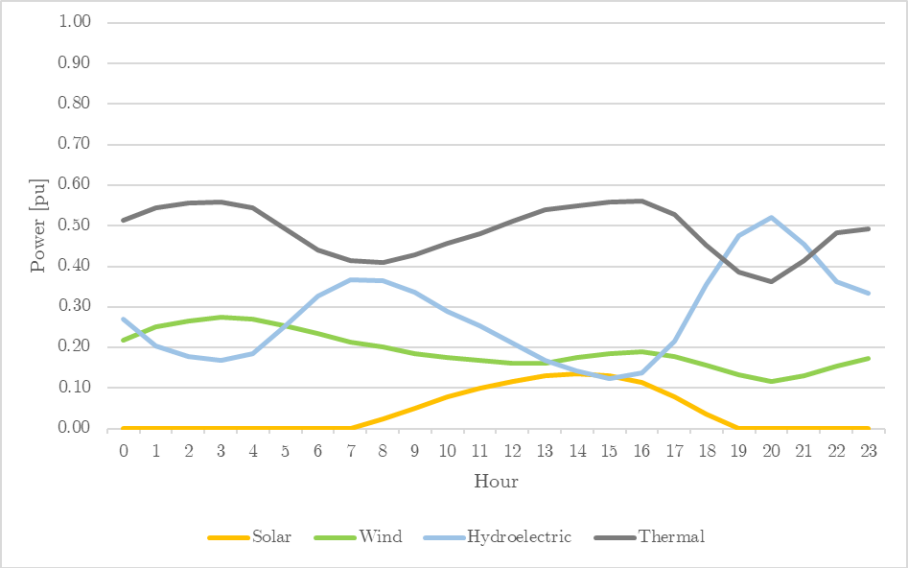

Figure 14: Average generation profile – May

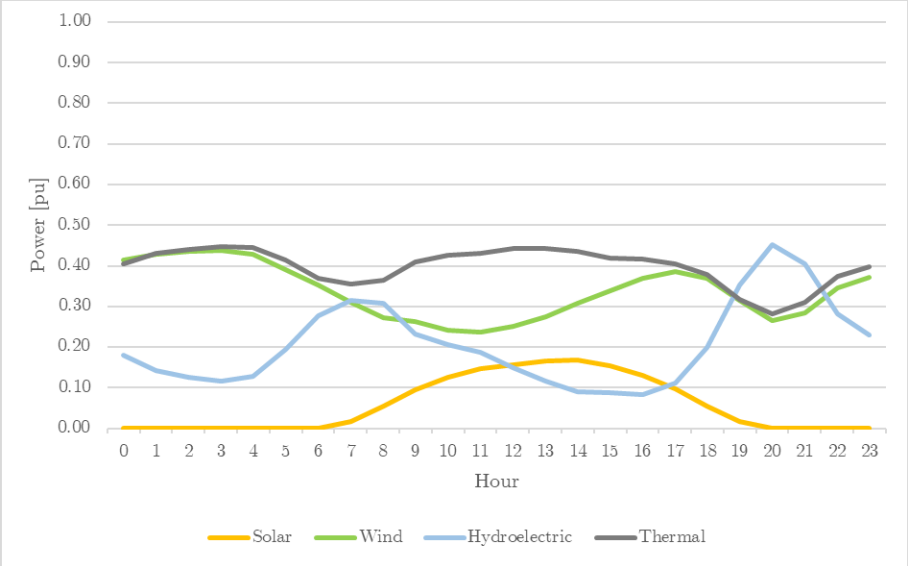

Figure 15: Average generation profile – June

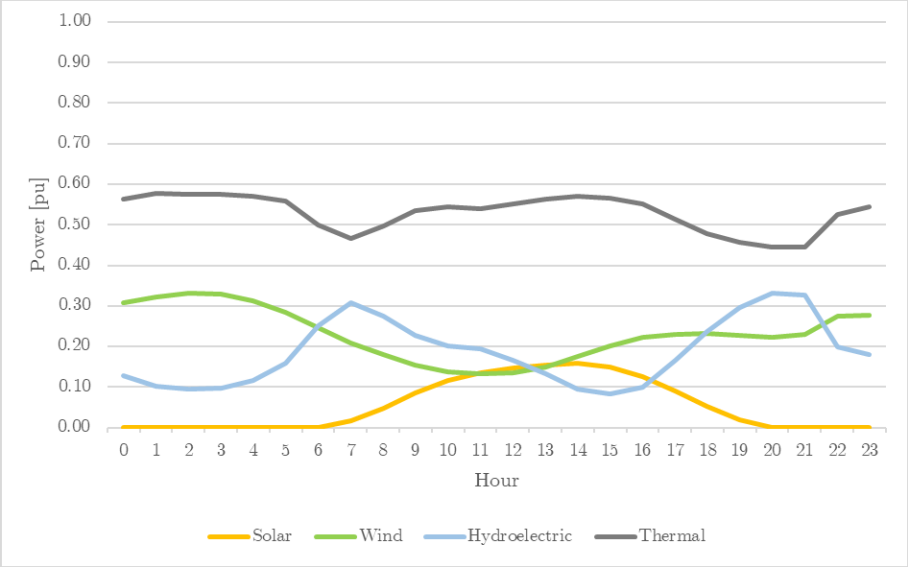

Figure 16: Average generation profile – July

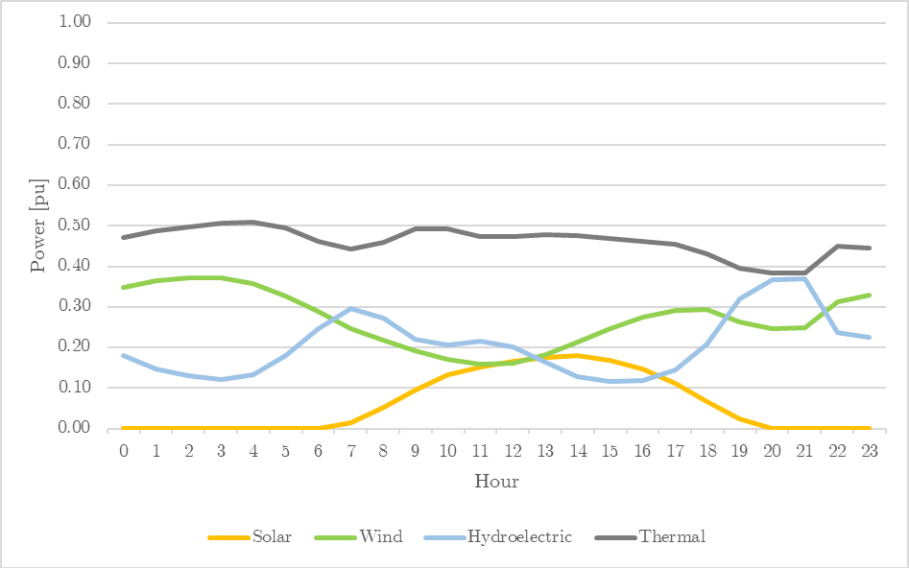

Figure 17: Average generation profile – August

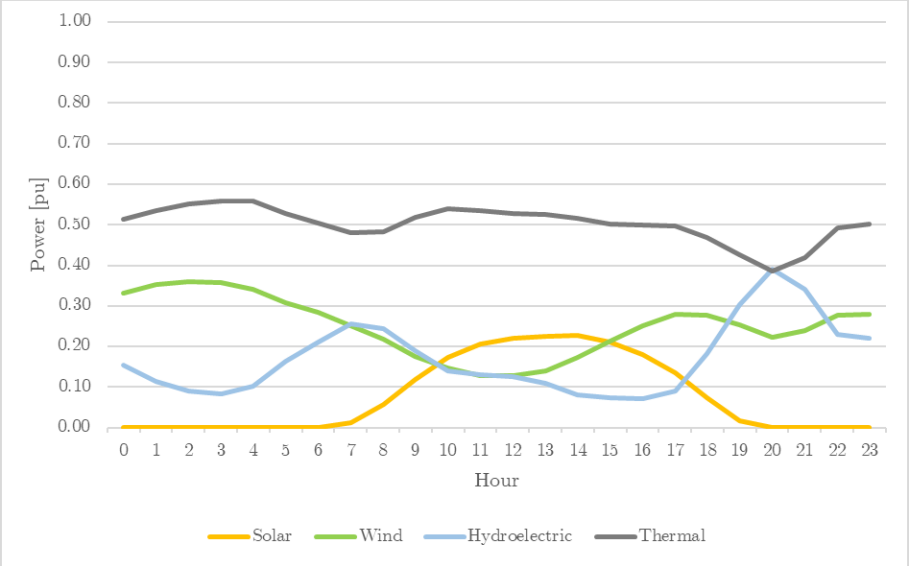

Figure 18: Average generation profile – September

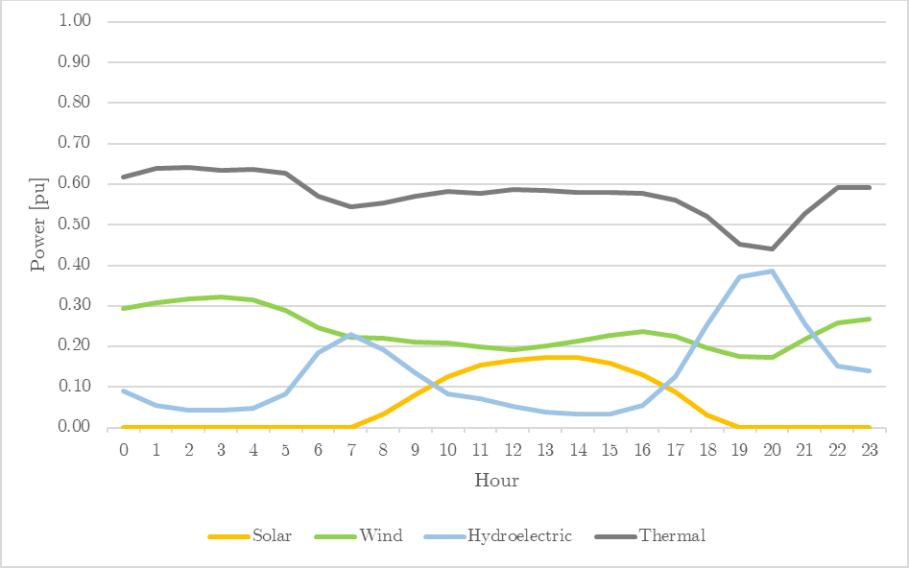

Figure 19: Average generation profile – October

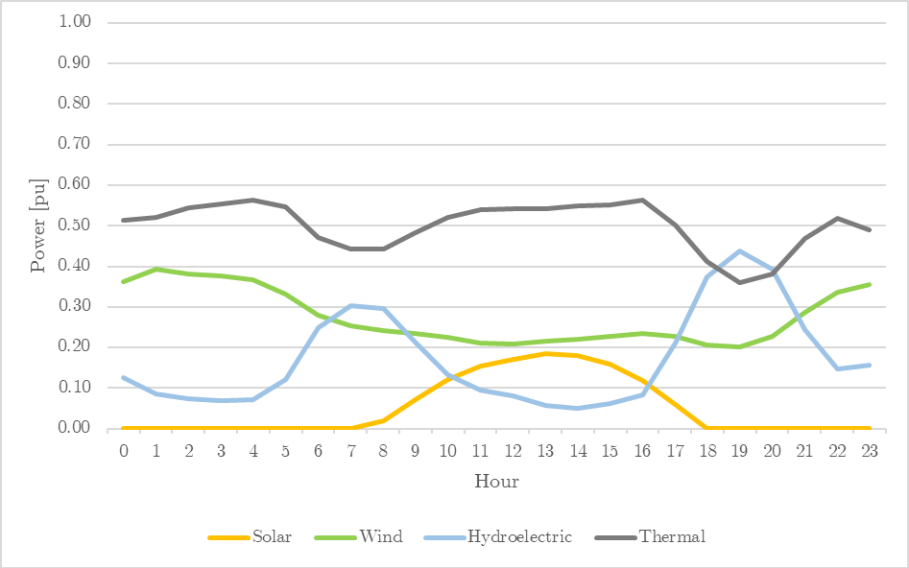

Figure 20: Average generation profile – November

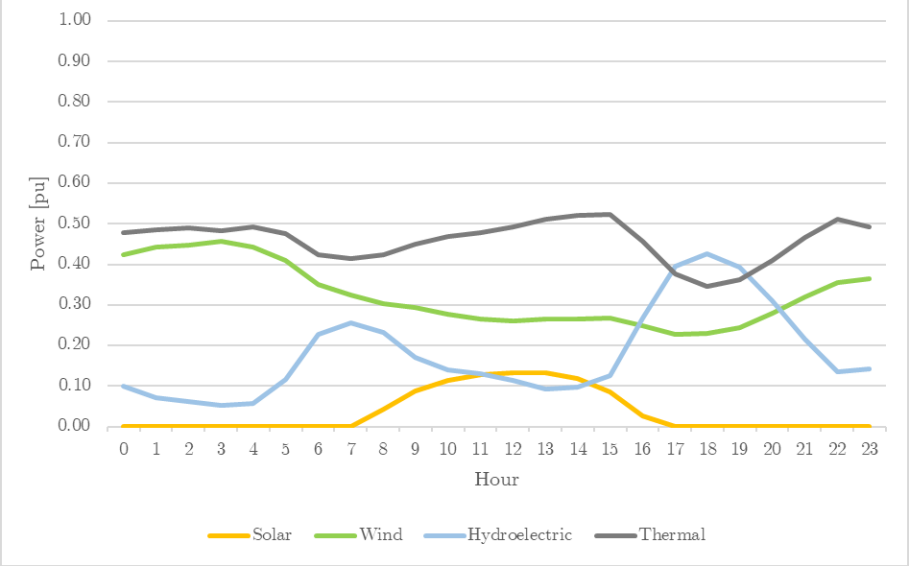

Figure 21: Average generation profile - December

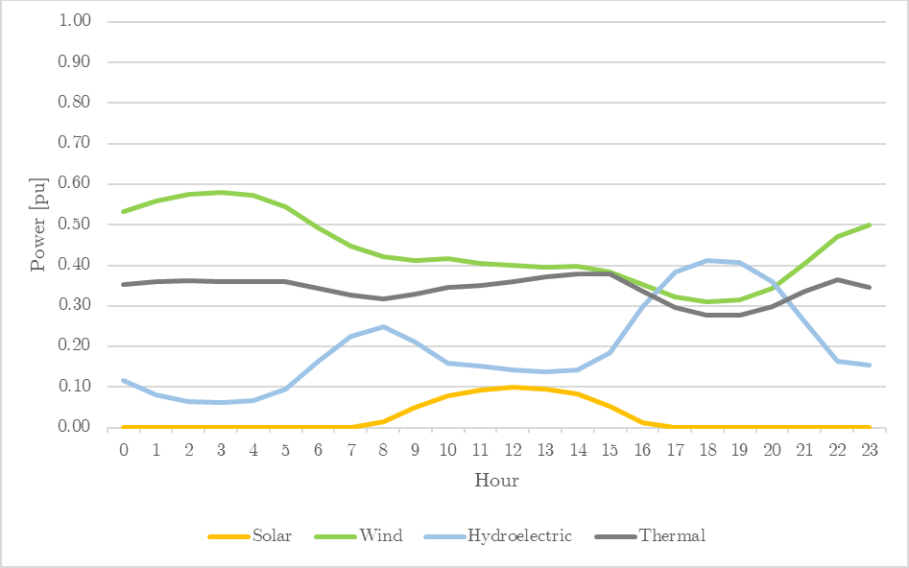

3.3 Transmission grid

A reduced transmission network model of 39 buses was used, specifically the IEEE-39, on the PSS®E tool. The model has 10 generators and 19 load nodes [43]. Modifications were made to the base model so that the representative cases could be incorporated into it. In its base form, this system has a demand of 5857 MW, which is less than the maximum demand for 2021, according to the data shown in section 3.2.1. Adjustments were made to the demand for it to scale properly to the available transmission network. The complete model of the network, and its parameters, will be shown in section 3.3.1. Section 3.3.2 will describe the procedure to adjust the operating scenarios obtained in section 3.2 so that they can be simulated with the available transmission grid.

3.3.1 Grid model

The model used differs from the base model in that transmission lines were added and their base capacity was modified to allow the information to be incorporated without provoking overloads that would interfere with the results. The one-line diagram in Figure 22 shows the network used. The parameters of the transmission lines and transformers in the grid are summarized in Table 1 and Table 2 respectively. This transmission network is generally meshed and presents few restrictions on power flows. It is also worth noting that the generation units are located in the outer buses of the network, while the central nodes are mainly destined to supply demand, and they do not have nearby generation sources. This characteristic is mentioned since the results will be highly dependent on the topology of the grid to be analyzed. Despite this, the results obtained are useful in their purpose of identifying the hosting capacity for the buses of a system and identifying the effect of using different rating adjustments for the elements in the network.

Ten generation units are available in the test system, the parameters of these units are shown in Table 3. The parameters of the units were modified to properly adapt to the operating cases built in previous steps. Specifically, the capacity of the machines was adjusted to maintain the consistency of the magnitude of the power to be delivered by them.

Table 1: Network parameters for transmission lines in the grid.

Bus *i*	Bus *j*	Circuit ID	r [pu]	x [pu]	b [pu]	Reference rating [MVA]
1	2	A	0.0035	0.0411	0.6987	418.7
1	2	B	0.0035	0.0411	0.6987	418.7
1	39	A	0.0010	0.0250	0.7500	207.1
1	39	B	0.0010	0.0250	0.7500	207.1

Bus i	Bus j	Circuit ID	r [pu]	x [pu]	b [pu]	Reference rating [MVA]
1	39	C	0.0010	0.0250	0.7500	207.1
2	3	A	0.0013	0.0151	0.2572	1072.5
2	3	B	0.0013	0.0151	0.2572	1072.5
2	25	A	0.0070	0.0086	0.1460	397.3
2	25	B	0.0070	0.0086	0.1460	397.3
2	25	C	0.0070	0.0086	0.1460	397.3
3	4	A	0.0013	0.0213	0.2214	226.0
3	4	B	0.0013	0.0213	0.2214	226.0
3	4	C	0.0013	0.0213	0.2214	226.0
3	18	A	0.0011	0.0133	0.2138	427.7
3	18	B	0.0011	0.0133	0.2138	427.7
3	18	C	0.0011	0.0133	0.2138	267.1
4	5	A	0.0008	0.0128	0.1342	782.4
4	14	A	0.0008	0.0129	0.1382	509.9
5	6	A	0.0002	0.0026	0.0434	853.6
5	8	A	0.0008	0.0112	0.1476	584.2
6	7	A	0.0006	0.0092	0.1130	885.5
6	11	A	0.0007	0.0082	0.1389	770.0
6	11	B	0.0007	0.0082	0.1389	770.0
7	8	A	0.0004	0.0046	0.0780	538.5
8	9	A	0.0023	0.0363	0.3804	512.0
8	9	B	0.0023	0.0363	0.3804	512.0
9	39	A	0.0010	0.0250	1.2000	440.0
9	39	B	0.0010	0.0250	1.2000	440.0
10	11	A	0.0004	0.0043	0.0729	762.0
10	11	B	0.0004	0.0043	0.0729	762.0
10	13	A	0.0004	0.0043	0.0729	712.9
13	14	A	0.0009	0.0101	0.1723	793.2
14	15	A	0.0018	0.0217	0.3660	366.4
14	15	B	0.0018	0.0217	0.3660	366.4
15	16	A	0.0009	0.0094	0.1710	754.0
15	16	B	0.0009	0.0094	0.1710	754.0
16	17	A	0.0007	0.0089	0.1342	595.0
16	17	B	0.0007	0.0089	0.1342	595.0
16	17	C	0.0007	0.0089	0.1342	595.0
16	19	A	0.0016	0.0195	0.3040	1165.0
16	19	B	0.0016	0.0195	0.3040	1165.0
16	21	A	0.0008	0.0135	0.2548	707.0
16	21	B	0.0008	0.0135	0.2548	707.0
16	24	A	0.0003	0.0059	0.0680	908.4
17	18	A	0.0007	0.0082	0.1319	670.0
17	18	B	0.0007	0.0082	0.1319	670.0
17	27	A	0.0013	0.0173	0.3216	363.3
17	27	B	0.0013	0.0173	0.3216	363.3

Bus i	Bus j	Circuit ID	r [pu]	x [pu]	b [pu]	Reference rating [MVA]
17	27	C	0.0013	0.0173	0.3216	363.3
21	22	A	0.0008	0.0140	0.2565	1073.0
21	22	B	0.0008	0.0140	0.2565	1073.0
22	23	A	0.0006	0.0110	0.1846	429.9
22	23	B	0.0006	0.0110	0.1846	429.9
22	23	C	0.0006	0.0110	0.1846	429.9
23	24	A	0.0022	0.0350	0.3610	770.0
25	26	A	0.0032	0.0323	0.5130	319.7
25	26	B	0.0032	0.0323	0.5130	319.7
25	26	C	0.0032	0.0323	0.5130	319.7
26	27	A	0.0014	0.0147	0.2396	418.0
26	27	B	0.0014	0.0147	0.2396	418.0
26	27	C	0.0014	0.0147	0.2396	418.0
26	28	A	0.0043	0.0474	0.7802	400.0
26	28	B	0.0043	0.0474	0.7802	400.0
26	29	A	0.0057	0.0625	1.0290	366.4
26	29	B	0.0057	0.0625	1.0290	366.4
28	29	A	0.0014	0.0151	0.2490	660.0
28	29	B	0.0014	0.0151	0.2490	660.0

Table 2: Network parameters for transformers in the grid.

Bus i	Bus j	Circuit ID	r [pu]	x [pu]	b [pu]	Reference rating [MVA]
11	12	A	0.0016	0.0435	0	436.4
12	13	A	0.0016	0.0435	0	323.4
12	13	B	0.0016	0.0435	0	323.4
19	20	A	0.0007	0.0138	0	483.0
19	20	B	0.0007	0.0138	0	483.0

Table 3: Machine parameters from test network

Bus	P_{max} [MW]	Q_{max} [MVAr]	Q_{min} [MVAr]	S_{base} [MVA]	R_{source} [pu]	X_{source} [pu]	Initial participation [%]
30	360.00	153.18	-58.08	275.00	0.0014	0.0079	4.2%
31	950.00	429.80	-122.67	836.00	0.0270	0.2978	9.7%
32	850.00	277.31	-277.31	843.70	0.0039	0.0257	11.0%
33	1068.00	386.14	-386.14	1174.80	0.0022	0.0080	10.7%
34	982.00	611.50	-188.03	1080.20	0.0014	0.0057	8.6%
35	987.00	356.85	-356.85	1085.70	0.0615	0.4654	11.0%
36	1100.00	568.37	-249.13	1025.20	0.0027	0.0214	9.5%
37	1100.00	318.89	-318.89	970.20	0.0069	0.0608	9.1%
38	1531.00	834.78	-356.89	1684.10	0.0030	0.0117	14.0%
39	1090.00	574.85	-173.26	1199.00	0.0010	0.0026	12.2%

Figure 22: Test network one-line diagram

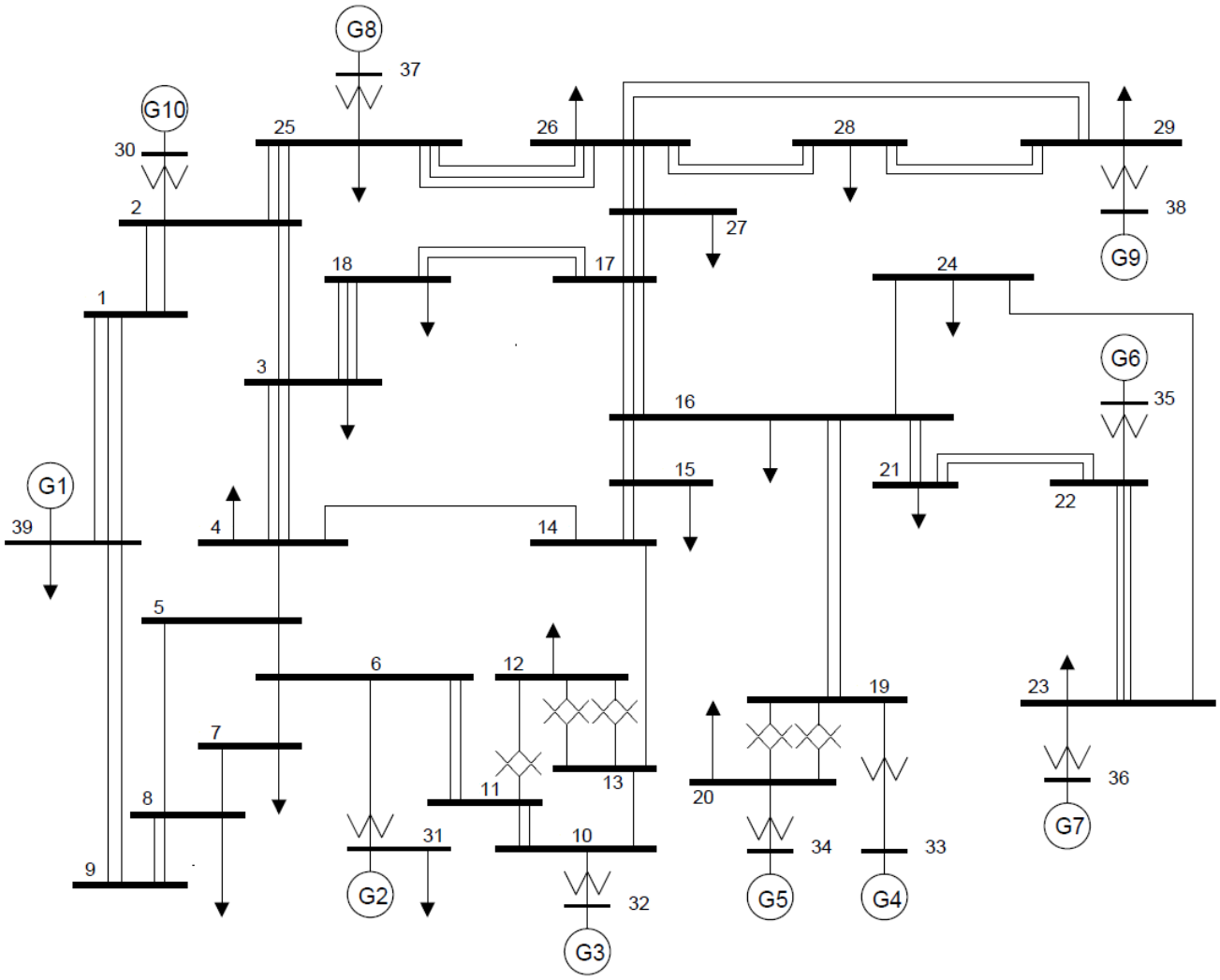

3.3.2 Incorporation of the operational scenarios to the grid model

3.3.2.1 Load

Considering that the demand in the test model is significantly lower than the maximum demand observed in the Portuguese system, it is necessary to make adjustments to be able to incorporate the operating scenarios built in section 3.2. The demand was scaled so that the maximum demand obtained from the current section corresponds to the demand in the initial test model. This same adjustment factor was used for all the demands of the year. The initial demand in the IEEE-39 test system was 5857 MW, while the maximum demand obtained from the operating scenarios was 8472.7 MW, the resulting scaling factor is 0.6846 pu. This factor was applied to the 288 hourly demands used. In this way, issues like numerical convergence and undesired overloads are avoided, situations that can alter the results obtained from the analysis. It is worth mentioning that this scaling factor does not alter seasonal or hourly variations of the demand, since it

is a uniform modification to all the values used, therefore, the behavior, patterns, and shape are consistent with those shown in the figures in section 3.2.1.

3.3.2.2 Generation

To represent the behavior of the generation, the patterns shown in section 3.2.2 was transferred to the generation units available in the model. As previously mentioned, generation was classified into four categories, thermal, hydroelectric, wind and solar. In terms of installed capacity by 2021, thermal units add up to 4,553 MW, 25% of the group, wind power plants 5,368 MW, equivalent to 29% of capacity, solar power plants add up to 1,387 MW, 7% of the mix, and hydroelectric power plants 7,222 MW representing 39% of the capacity.

As shown in Table 3, there are ten generation units available in the test network, for which it is necessary to match the available units and assign them a specific technology, so that the percentages of installed capacity are similar between the available model and the actual information. The assignment was made through a combination of units that add an equivalent power, as a percentage, to the installed power in the system of each technology. The allocation used is summarized in Table 4. Following the sequence for the model, the thermal units add up to 2981 MW, which is equivalent to 30% of the total, the unit assigned as solar has a capacity of 950 MW, which represents 9% of the total. Hydroelectric units total 3,887 MW, which is 39% of the total. Finally, the wind units total 2,200 MW or 22% of the total. While the percentages do differ, they provide a reasonable quota for the analysis. This step would not be necessary for a real system, since it would be possible to use the real capacity for each plant in the system. Table 5 shows a comparison of the participation of the installed capacity in both situations, the real information of the Portuguese system and the information scaled to the test system.

Table 4: Unit assignment by technology

Bus	Name	Technology	P_{Max} [MW]
30	Thermal 3	Thermal	360
31	Solar	Solar	950
32	Hydro 1	Hydroelectric	850
33	Hydro 2	Hydroelectric	1068
34	Hydro 3	Hydroelectric	982
35	Hydro 4	Hydroelectric	987
36	Wind 1	Wind	1100
37	Wind 2	Wind	1100
38	Thermal 1	Thermal	1531
39	Thermal 2	Thermal	1090

Table 5: Participation of installed capacity

Technology	Real data [MW]		Test network [MW]	
	Capacity [MW]	Participation [%]	Capacity [MW]	Participation [%]
Thermal	4553	25%	2981	30%
Solar	1387	7%	950	9%
Hydroelectric	7222	39%	3887	39%
Wind	5368	29%	2200	22%

The previous step only allows the units to be assigned to each of the technologies in such a way that the proportion of them is maintained in terms of installed capacity. The next step is to identify how much of the total production by technology will be assigned to each corresponding unit. For this, the initial participation factor shown in Table 3 is taken into account.

As an example, to identify the participation of one of the thermal units, its initial participation is divided by the total participation of the units marked with the same technology in the assignment of the previous step. In this case, Table 3 shows that the unit at bus 30 has an initial participation of 4.2%, while units 38 and 39 have an initial participation of 14.0 and 12.2% respectively. For the unit in bus 30, its individual participation is calculated as follows:

$$ip_{30} = \frac{4.2\%}{4.2\% + 14.0\% + 12.2\%} = 13.9\%$$

This indicates that the unit at node 30 will contribute 13.9% of the total thermal generation for a particular hour. This procedure is repeated for the other units and technologies, the results of individual participation are summarized in Table 6.

Table 6: Technology participation by individual unit

Bus	Unit	Initial participation [%]	Technology participation [%]
34	Hydro 3	8.6%	20.8%
35	Hydro 4	11.0%	26.6%
32	Hydro1	11.0%	26.6%
33	Hydro2	10.7%	25.9%
31	Solar	9.7%	100.0%
38	Thermal 1	14.0%	46.1%
39	Thermal 2	12.2%	40.0%
30	Thermal 3	4.2%	13.9%
36	Wind 1	9.5%	50.9%
37	Wind 2	9.1%	49.1%

It is possible, with the participation by technology shown in section 3.2.2, to calculate how much generation each unit will contribute for all the operating scenarios used. This makes it possible to reflect the individual conditions of each technology and their variations throughout the year, as well as the expected hourly variations due to their technical characteristics. Again, the use of these scaling factors does not affect the general behavior of production since the homogeneous adjustment, therefore, the patterns of each technology are preserved and remain useful for the analysis.

3.4 Rating adjustment factors

As mentioned in previous sections, three types of adjustment to the transmission line rating were used. A static setting where the capacity of the transmission lines is constant throughout the year. It is common to consider severe or adverse environmental conditions to calculate the rating, this is to proceed with caution and avoid undesired overestimations of transmission line capacity. This setting is called Static Line Rating (SLR).

The second factor considered was a seasonal adjustment, in this case, a transmission capacity scaling factor was calculated, considering average environmental conditions for each month of the year. For this adjustment factor, the variation occurs in the ambient temperature taken as a reference. It is expected that during the winter months, when the ambient temperature is significantly lower, the conductors can carry a higher current without compromising their integrity. This mechanism is called Seasonal Adjustment Rating (SAR). The seasonal adjustment factors used are shown in Table 7 and Figure 23

Table 7: Seasonal Adjustment Rating factors

Month	SAR [pu]
Jan	1.0957
Feb	1.0957
Mar	1.0957
Apr	1.0665
May	1.0427
Jun	1.000
Jul	1.000
Aug	1.000
Sep	1.000
Oct	1.0345
Nov	1.0705
Dec	1.0957

Figure 23: Comparison of SLR and SAR adjustment factors

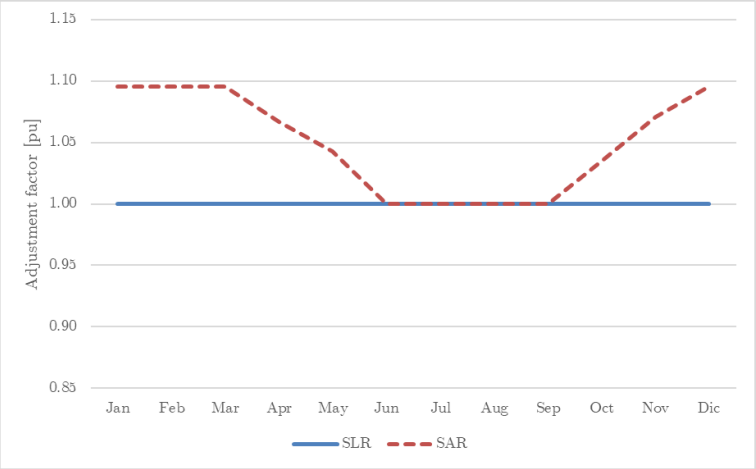

Hourly factors are used to increase the resolution of the rating adjustment. The day is divided into three zones, or time slots, which correspond to dawn, daytime and nighttime. The first band corresponds to the daytime, in which a reference temperature and a solar radiation of 1000 W/m^2 are considered. The second time slot corresponds to nighttime, after sunset. The variation consists in not include the effect of solar radiation, and the reference temperature is kept the same. For dawn, called band 3, a reference temperature 5°C lower than the temperature of the other bands is considered, and zero solar radiation. It is necessary to mention that the duration of the time slots is not uniform since they must reflect the behavior of sunrise and sunset for each month of the year. The mapping of the time slots is shown in Table 8.

Table 8: Hour zone mapping for AAR

Hour \ Month	Jan	Feb	Mar	Apr	May	Jun	Jul	Aug	Sep	Oct	Nov	Dec
0	3	3	3	3	3	3	3	3	3	3	3	3
1	3	3	3	3	3	3	3	3	3	3	3	3
2	3	3	3	3	3	3	3	3	3	3	3	3
3	3	3	3	3	3	3	3	3	3	3	3	3
4	3	3	3	3	3	3	3	3	3	3	3	3
5	3	3	3	3	3	1	3	3	3	3	3	3
6	3	3	3	1	1	1	1	1	3	3	3	3
7	3	3	1	1	1	1	1	1	1	1	3	3
8	1	1	1	1	1	1	1	1	1	1	1	1
9	1	1	1	1	1	1	1	1	1	1	1	1
10	1	1	1	1	1	1	1	1	1	1	1	1
11	1	1	1	1	1	1	1	1	1	1	1	1
12	1	1	1	1	1	1	1	1	1	1	1	1
13	1	1	1	1	1	1	1	1	1	1	1	1
14	1	1	1	1	1	1	1	1	1	1	1	1
15	1	1	1	1	1	1	1	1	1	1	1	1
16	1	1	1	1	1	1	1	1	1	1	1	1
17	1	1	1	1	1	1	1	1	1	1	1	1
18	2	2	1	1	1	1	1	1	1	2	2	2
19	2	2	2	2	1	1	1	1	2	2	2	2
20	2	2	2	2	2	2	2	2	2	2	2	2
21	2	2	2	2	2	2	2	2	2	2	2	2
22	2	2	2	2	2	2	2	2	2	2	2	2
23	2	2	2	2	2	2	2	2	2	2	2	2

After classifying it into time slots, a relationship is established between the daytime and nighttime capacity of each month. Capacity estimates are made

considering the monthly reference temperature and the premises of each time slot. Table 9 shows the factors used for each time band relative to time band 1, this is taken as the baseband because it considers the highest reference temperature and highest solar radiation, which are usual conditions for calculating the static rating. in transmission lines.

Table 9: Rating ratios for monthly hour zones

Month	T_{ref} [°C]	Zone 1	Zone 2/Zone 1	Zone 3/ Zone 1
Jan	15	1.00	1.08	1.12
Feb	15	1.00	1.08	1.12
Mar	15	1.00	1.08	1.12
Apr	20	1.00	1.09	1.13
May	25	1.00	1.09	1.15
Jun	30	1.00	1.11	1.16
Jul	30	1.00	1.11	1.16
Aug	30	1.00	1.11	1.16
Sep	30	1.00	1.11	1.16
Oct	25	1.00	1.09	1.15
Nov	20	1.00	1.09	1.13
Dec	15	1.00	1.08	1.12

The factors in Table 9 only show the variation between daytime to nighttime or daytime to dawn for a particular month. These do not capture the monthly variations themselves, for this it is necessary to combine them with the seasonal factors shown in Table 7. Multiplying the zone factor with the factor of the corresponding month it is possible to obtain a mapping for the 24 hours of the day for each month, the result of this procedure is summarized in Table 10. To further show the effect of considering the time adjustments, the summary table is complemented by the graphs shown from Figure 24 to Figure 27.

Table 10: Hourly adjustment factor for AAR

Hour \ Month	Jan	Feb	Mar	Apr	May	Jun	Jul	Aug	Sep	Oct	Nov	Dec
0	1.23	1.23	1.23	1.21	1.19	1.16	1.16	1.16	1.16	1.19	1.21	1.23
1	1.23	1.23	1.23	1.21	1.19	1.16	1.16	1.16	1.16	1.19	1.21	1.23
2	1.23	1.23	1.23	1.21	1.19	1.16	1.16	1.16	1.16	1.19	1.21	1.23
3	1.23	1.23	1.23	1.21	1.19	1.16	1.16	1.16	1.16	1.19	1.21	1.23
4	1.23	1.23	1.23	1.21	1.19	1.16	1.16	1.16	1.16	1.19	1.21	1.23
5	1.23	1.23	1.23	1.21	1.19	1.16	1.16	1.16	1.16	1.19	1.21	1.23
6	1.23	1.23	1.23	1.21	1.19	1.00	1.16	1.16	1.16	1.19	1.21	1.23
7	1.23	1.23	1.10	1.07	1.04	1.00	1.00	1.00	1.16	1.19	1.21	1.23
8	1.10	1.10	1.10	1.07	1.04	1.00	1.00	1.00	1.00	1.03	1.07	1.10
9	1.10	1.10	1.10	1.07	1.04	1.00	1.00	1.00	1.00	1.03	1.07	1.10
10	1.10	1.10	1.10	1.07	1.04	1.00	1.00	1.00	1.00	1.03	1.07	1.10
11	1.10	1.10	1.10	1.07	1.04	1.00	1.00	1.00	1.00	1.03	1.07	1.10
12	1.10	1.10	1.10	1.07	1.04	1.00	1.00	1.00	1.00	1.03	1.07	1.10
13	1.10	1.10	1.10	1.07	1.04	1.00	1.00	1.00	1.00	1.03	1.07	1.10
14	1.10	1.10	1.10	1.07	1.04	1.00	1.00	1.00	1.00	1.03	1.07	1.10
15	1.10	1.10	1.10	1.07	1.04	1.00	1.00	1.00	1.00	1.03	1.07	1.10
16	1.10	1.10	1.10	1.07	1.04	1.00	1.00	1.00	1.00	1.03	1.07	1.10
17	1.10	1.10	1.10	1.07	1.04	1.00	1.00	1.00	1.00	1.03	1.07	1.10
18	1.18	1.18	1.10	1.07	1.04	1.00	1.00	1.00	1.00	1.03	1.16	1.18
19	1.18	1.18	1.18	1.07	1.04	1.00	1.00	1.00	1.00	1.13	1.16	1.18
20	1.18	1.18	1.18	1.16	1.04	1.00	1.00	1.00	1.11	1.13	1.16	1.18
21	1.18	1.18	1.18	1.16	1.14	1.11	1.11	1.11	1.11	1.13	1.16	1.18
22	1.18	1.18	1.18	1.16	1.14	1.11	1.11	1.11	1.11	1.13	1.16	1.18
23	1.18	1.18	1.18	1.16	1.14	1.11	1.11	1.11	1.11	1.13	1.16	1.18

Figure 24: Hourly adjustment factors – Winter

Figure 25: Hourly adjustment factors – Spring

Figure 26: Hourly adjustment factors – Summer

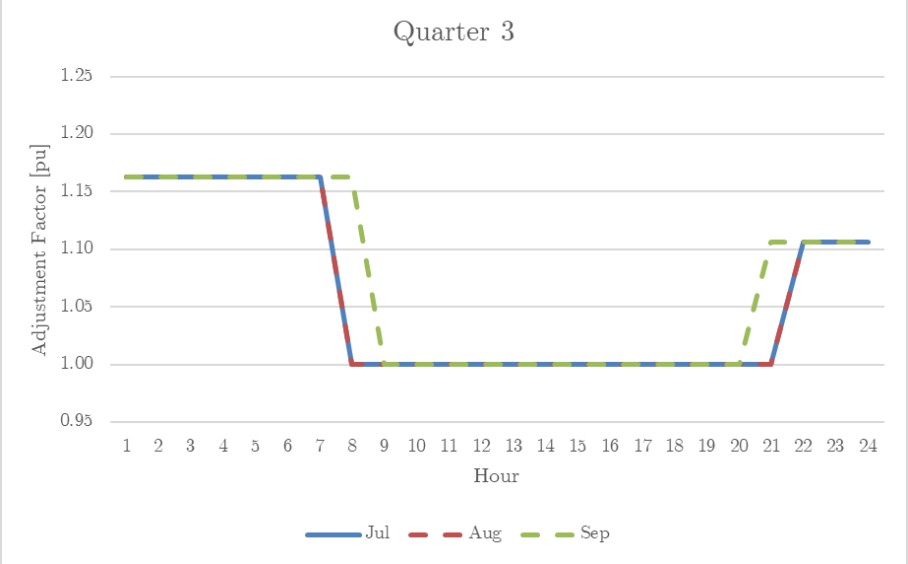

Figure 27: Hourly adjustment factors – Autumn

From Figure 23 and Figure 24 to Figure 27 it is noticeable the advantage in considering seasonal or hourly factors. With seasonal adjustment (SAR), an increase close to 10% in the rating is observed for the winter months compared to the summer months. This behavior is only accentuated when considering the hourly adjustments since the increase in transport capacity can exceed the reference value by 18% during winter nighttime and 11% for summer nighttime, which are usually times of high system load. Therefore, it is less likely to encounter restrictions in the transmission grid when using more detailed assumptions in the estimations of the rating of transmission lines.

3.5 Assembly of operational scenarios in PSS®E

Considering the treatment carried out on the information, which was described in sections 3.2 to 3.4, the following step is to incorporate the operating scenarios into a PSS®E model of the transmission network to be used. 288 study cases were built, and the operating conditions and load of the circuits were verified before carrying out the power additions considered in the analysis. The slight deviations caused by the losses in the transmission network were compensated by the slack unit in the system, in this case, the designated unit was the one located in bus 38.

The solution method used initially is the decoupled Newton-Raphson, this method was used due to its precision and the reduction in computational effort. The individual differences in using the complete or decoupled method may be negligible for a particular case, but by increasing the number of iterations necessary to calculate the power flows, the time difference begins to be significant. In this initial stage, the adjustment of the tap controller in the existing transformers was allowed to avoid voltage control problems that cause abnormal flows of reactive power that could contaminate the results.

When performing power additions, it is not appropriate to use the same solution method since power variations, both in generation and demand, are completely absorbed by the slack unit. This is an unrealistic case for the actual operation of an electrical system, where significant changes in generation will require dispatch according to current conditions. To consider these conditions, the governor dispatch method is used. Although, indeed, the method is not designed for this purpose, it is possible to use said solution mechanism to compensate for the changes in generation and demand with the units that would see an impact on their output. For this redispatch process, the units that correspond to solar and wind technologies were excluded, which due to their characteristics do not allow their output power to be modified easily at will. In

this case, it is considered that the thermal and hydroelectric units modify their output to accommodate the power additions that are carried out in the tests. The information needed to solve the governor-based power flow is summarized in Table 11. Specifically, the droop characteristic and governor type are required. Solar and wind units are excluded from this solution mechanism by setting the maximum power P_{max} equal to the minimum power P_{min}. For thermal units, a generic governor for steam turbines and cylindrical rotor is used, while for hydroelectric units, a generic governor for hydraulic turbines and a salient rotor of the generator is considered [44] [45].

Table 11: Governor and inertial characteristics for power flow solution

Bus	Name	H [pu]	P_{max} [pu]	P_{min} [pu]	Droop [pu]	Damping [pu]	Rotor type	Governor
30	Thermal 3	4	1	0	0.05	0	Cylindrical	TGOV1
31	Solar	4	1	1	0.05	0	Salient	HYGOV
32	Hydro 1	4	1	0	0.05	0	Salient	HYGOV
33	Hydro 2	4	1	0	0.05	0	Salient	HYGOV
34	Hydro 3	4	1	0	0.05	0	Salient	HYGOV
35	Hydro 4	4	1	0	0.05	0	Salient	HYGOV
36	Wind 1	4	1	1	0.05	0	Salient	HYGOV
37	Wind 2	4	1	1	0.05	0	Salient	HYGOV
38	Thermal 1	4	1	0.3	0.05	0	Cylindrical	TGOV1
39	Thermal 2	4	1	0.3	0.05	0	Cylindrical	TGOV1

Finally, it is necessary to calculate the power flows in the N-1 condition. In this case, the decoupled Newton-Raphson method is used again due to generation contingencies not being considered. The changes in the losses are absorbed by the slack unit without a significant impact on the results. Another consideration was blocking the tap controller in the transformers in the network since the actuation times of this mechanism are usually high, relative to changes in power flows after a contingency.

3.6 Operational security criteria

For the analysis, it is necessary to set the accepted loading for the transmission lines in each operational condition, either steady state in N-0 condition, or N-1 condition. For the first condition, where all the elements are in service, an overload is set as a current flow greater than 100% of the element's capacity, whether in the static, seasonal or hourly limit. For the N-1 condition, a power flow that represents 110% of the element's current capacity will be considered an overload.

3.7 General considerations

For the simulation, tests were carried out on all the buses in the grid, except for those that already have a generator connected. This results in 29 candidate buses for whom the hosting capacity was calculated.

Regarding the contingencies used, the disconnection of all transmission lines and transformers was considered, except for the transformers that link a generator with the high-voltage bus, since this would be categorized as a generation contingency. For the parallel elements shown in both Figure 22 and Table 1, only one of them was disconnected, since the contingencies of the second or third element are equivalent to each other, and therefore do not provide further information to the analysis. This consideration applies when the line impedances and electrical characteristics are equal. If that is not the case, it is advisable to analyze the contingencies separately as the power flows could behave differently.

For all test nodes, injections were made in the range of 400 MW to 900 MW with 100 MW increments. Initially, nodes were found that could accommodate 900 MW, for these nodes the injected power P_n was increased up to 1500 MW also in steps of 100 MW.

4 Results

This section includes the results obtained from implementing the methodology described in Chapter 3. The results obtained allow us to analyze different aspects, in addition to the main result, which is to identify the hosting capacity of each node in the network. The additional aspects, or secondary results are:

- The effect of the adjustments to the line rating on the hosting capacity, and the number of scenarios with overloads in the system.
- Sensitivity of hosting capacity to variations in tolerance
- Identification of elements or areas susceptible to network congestion in the event of power additions
- Changes in the seasonality of the overloads when considering the adjustments to the transport capacity

4.1 Hosting capacity

Initially, a tolerance h_{tol} equivalent to 1% of the total hours in a year was considered, which for this period is equivalent to 88 hours. Taking into account a sample size of 288 scenarios, the tolerance is equivalent to 2 samples in which it is admissible to identify overloads in N-0 and N-1 conditions. Therefore, the criterion can be expressed as $h_{N-0_{\%}} + h_{N-1_{\%}} < 1\%$ or $h_{N-0_m} + h_{N-1_m} < 2$, where the subscripts % and m refer to a percentage tolerance or a tolerance relative to the sample size, respectively. The results for the hosting capacity under the indicated tolerance are shown in Figure 28 and Table 12. These compare the hosting capacity for the three transport capacity settings used, SLR, SAR and AAR.

For some nodes, adjusting the rating does not have a significant effect on the maximum power that they can host. This applies to nodes 1, 5-8, 11-14 and 26-29. Based on the topology of the transmission network it is feasible to identify the possible causes of the restrictions in individual hosting capacity. Although the adjustments to the line rating do not seem to affect the hosting capacity in these buses, the difference in the number of hours h_{N-0} and h_{N-1} will be shown in later sections.

Bus 1, is located between two buses that receive power from existing plants in the system, and has limited options to evacuate additional power, especially if the new power in bus 1 is combined with the one injected by the units in buses 30 and 39. A similar case occurs with buses 26 to 29, where buses 26, 28 and 29 form an almost radial corridor between them, therefore, injections will be restricted

since said corridor must transport the production of the unit in bus 38, in combination with the new unit in one of the candidate buses.

Buses 5 to 8 are neighbors to each other, and have simple links between them, so a contingency in one of the links restricts the area's capacity to evacuate the possible generation incorporated in these nodes.

As for buses 11-13, they are located in the vicinity of two units, at bus 31 and 32. Unit 32 corresponds to hydroelectric technology, while unit 31 was assigned as the solar power plant. The combination of these two units and the candidate plant limits the capacity of this zone to evacuate the total injected power. Regarding bus 14, it has links to three neighboring nodes, but these correspond to a single link to bus 4 and another to bus 13, it also has a double link to bus 15. It is expected that the power on link 13-14 flows from node 13 to node 14, restricting the possible evacuation routes for any additional generation in the latter node.

On the contrary, buses 2-4, 9, and 15-25 show differences regarding the implementation of seasonal or hourly adjustments. For buses 2 and 3, there is an increase of 200 MW when considering SAR or 300 MW when for AAR compared to using only SLR. Bus 4 shows an increase of 200 MW for both adjustments, SAR and AAR, relative to the limit found using SLR. Buses 2-4 are part of a corridor with redundant links between them, and alternate evacuation routes, which allow the power injected into these nodes to be transported. Bus 2 is connected to the unit at node 30, which affects how much total power these neighboring nodes can host.

The most significant differences are observed in buses 15 to 19, where the increase reaches 500 MW for bus 15, and 800 MW for buses 16 and 17, while for buses 18 and 19 an increase of at least 400 MW is observed using the seasonal adjustment, and 500 and 600 MW respectively using AAR. Buses 15 to 18 are in the central area of the network, according to the diagram in Figure 22, in which it can be seen that these nodes have redundant links between them and the rest of the system. Also, this area of the network does not have existing power plants, so the candidate additions are not forced to share the existing transmission infrastructure. The combination of these factors means that even in the case of a simple contingency, the area does not see its ability to transport energy to the rest of the system significantly reduced.

Bus 19 does not meet the prior description, since it is located near the units at buses 33 and 34. However, this bus has the characteristic of having redundant

links to buses 16 and 20. Towards bus 16 the links have a rating of more than 1100 MVA each in their static condition, while the transformers between buses 19-20 have a rating of 483 MVA. This means that even with a contingency of one of these elements, the three remaining elements are capable of evacuating the generation injected into the area. These conditions improve when considering the SAR and AAR factors, since the capacity of the links in the network increases, especially in the winter months and at night.

It is clear that the results will depend on the transmission grid that is analyzed, however, these observations allow us to identify the effect of the network topology on the individual hosting capacity of each node and visualize the most suitable areas for the installation. of new power plants in the system, or the areas that require reinforcements to host additional power.

Table 12: Hosting capacity for $h_{tol_{\%}} = 1\%$

Bus	Hosting capacity [MW]		
	SLR	SAR	AAR
1	400	400	400
2	700	900	1000
3	600	800	900
4	700	900	900
5	400	400	400
6	400	400	400
7	400	400	400
8	400	400	400
9	400	400	500
10	400	400	400
11	400	400	400
12	300	300	300
13	400	400	400
14	400	400	400
15	700	1200	1200
16	700	1500	1500
17	700	1500	1500
18	700	1100	1200
19	700	1100	1300
20	600	600	700
21	300	400	400
22	300	400	500
23	400	500	600
24	700	800	900
25	500	700	800
26	500	500	500
27	500	500	500
28	500	500	500
29	500	500	500

Figure 28: Hosting capacity for $h_{tol_{\%}} = 1\%$

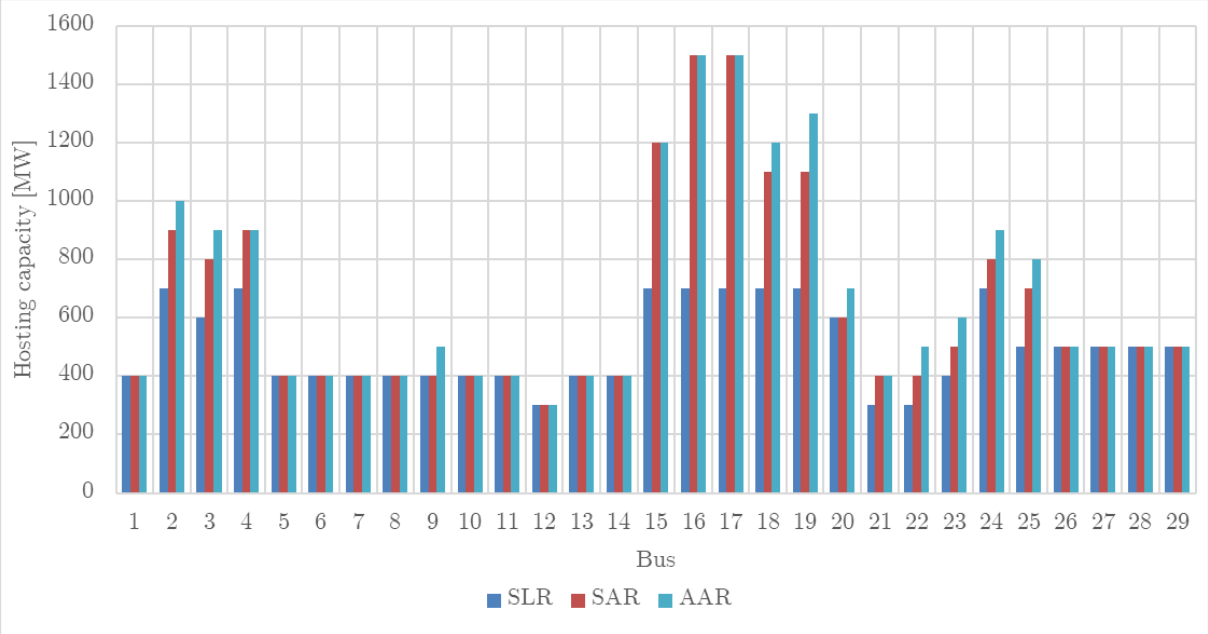

4.2 Impact of the hourly and seasonal adjustments

The selection criteria to identify the hosting capacity was the number of hours, or scenarios, h_{nP} for which overloads are registered under power injections P, in a node n of the system. It is expected that the number of overloads is dependent on the rating of the elements in the grid.

To analyze in greater detail, the impact of seasonal and hourly adjustments, SAR and AAR on h_{nP}, the number of overloads registered due to power injections in the range of 400 MW up to 900 MW or 1000 MW. The use of more specific adjustments for transport capacity estimates is compared based on h_{nP}. Figure 29 shows the number of scenarios with overloads for different power injections at each node, comparing the static, seasonal and hourly ratings.

In all the nodes the trend is notorious, h_{nP} for each adjustment factor decrease depending on the detail with which the transmission capacity is estimated. In general terms there is a corresponding value of h_{nP} for each capacity setting, these will be called $h_{nP_{SLR}}$, $h_{nP_{SAR}}$, and $h_{nP_{AAR}}$. For all the buses and power values shown, the relation $h_{nP_{SLR}} \geq h_{nP_{SAR}} \geq h_{nP_{AAR}}$ is fulfilled, this indicates that under all the analyzed combinations the adjustment factors do not have a negative impact on the number of scenarios under which overloads are recorded.

Apart from the relationship $h_{nP_{SLR}} \geq h_{nP_{SAR}} \geq h_{nP_{AAR}}$ no particular pattern is observed in the trend of the values h_{nP} recorded. For some buses such as 4-6, 10-11 and 13-14 it is observed that the improvements from using AAR relative to SAR are marginal or null since the number of scenarios $h_{nP_{SAR}}$ and $h_{nP_{AAR}}$ is the

same for the analyzed power injections. However, both settings show significant improvements over the use of a static limit on the rating. For another set of buses 1, 3, 8-9, 12 and 20-29, an improvement is observed in using SAR relative to SLR, and also an improvement in using AAR relative to SAR.

While it is true that the differences may not be enough to cause changes in hosting capacity, there is an impact of using variable adjustments to the line rating. The impact lies in eliminating transmission restrictions for the dispatch, which in principle allows a more economical dispatch. Another result of the implementation of variable adjustments is the possibility of delaying investments in the transmission grid or prioritizing investments in areas that show restrictions due to the typical environmental conditions of the area. Once again, it is considered necessary to emphasize that the magnitude of the benefits will depend on the topology of the transmission network, the dispatch conditions of the plants installed in the system, the merit order resulting from the optimization and other factors associated with the operation of an electrical system. Despite this, it is important to show the potential benefits of implementing changes to the transmission network models, especially if these do not represent a high cost in their implementation.

Figure 29: Comparison of h_{nP} for SLR, SAR and AAR at different injection levels

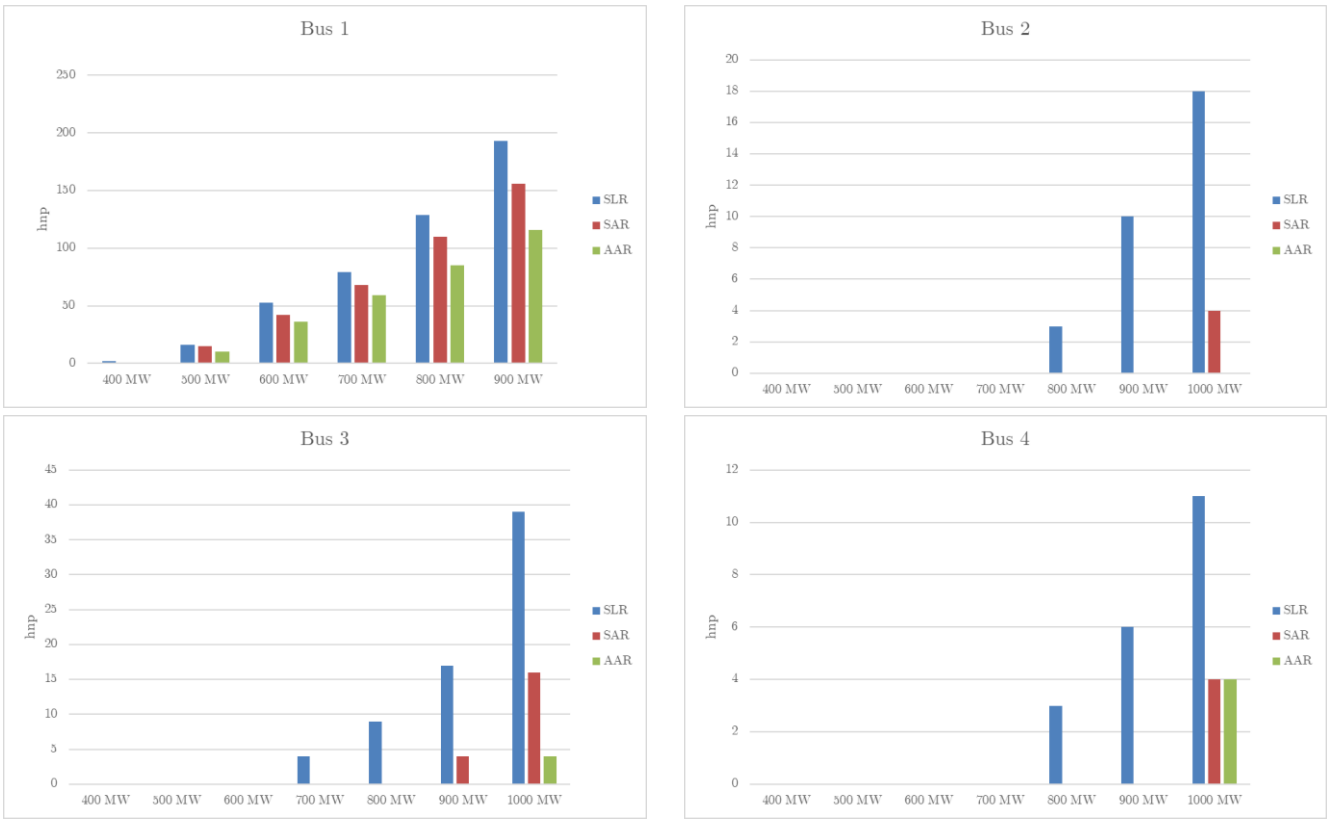

Figure 29: Comparison of h_{nP} for SLR, SAR and AAR at different injection levels

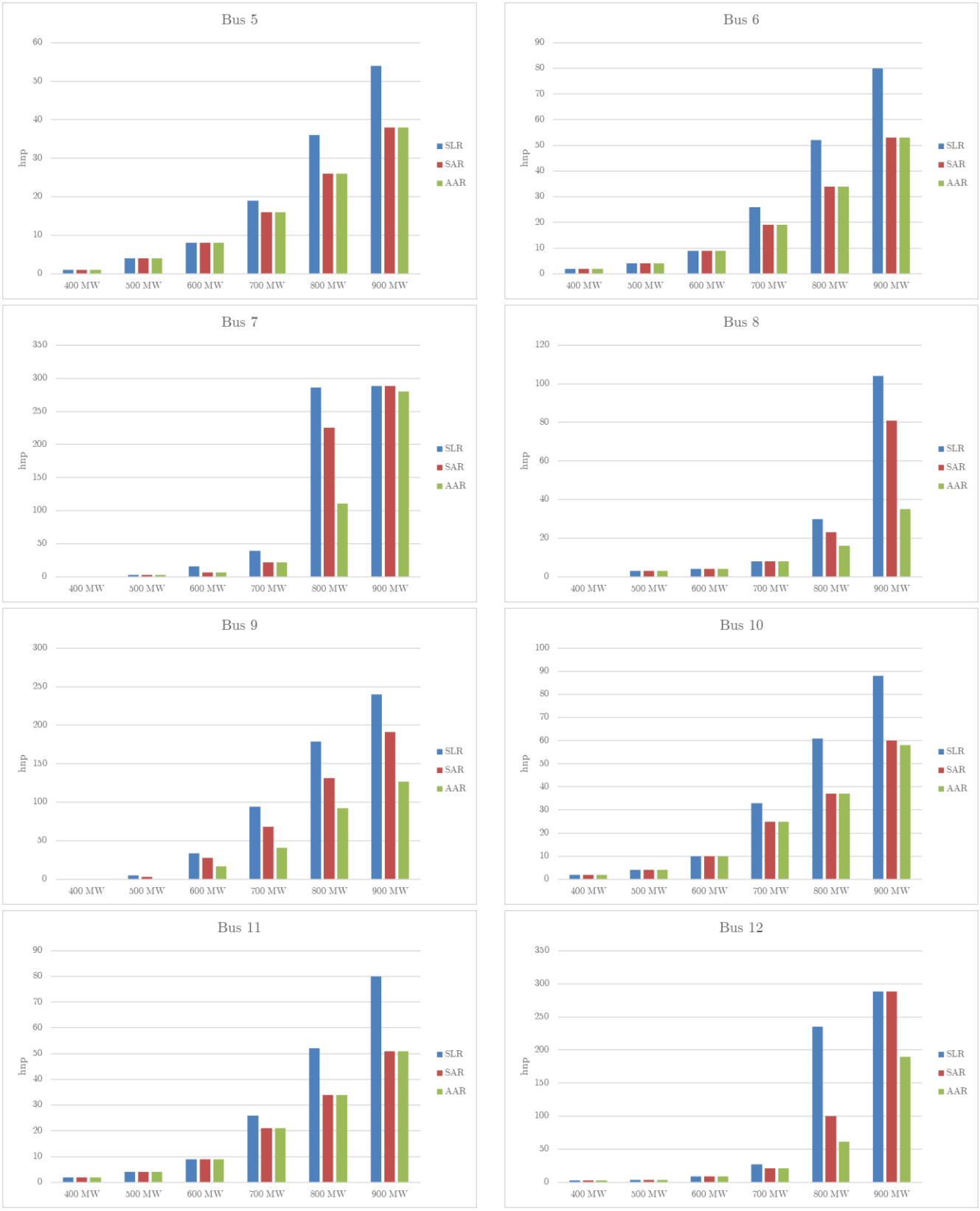

Figure 29: Comparison of h_{nP} for SLR, SAR and AAR at different injection levels

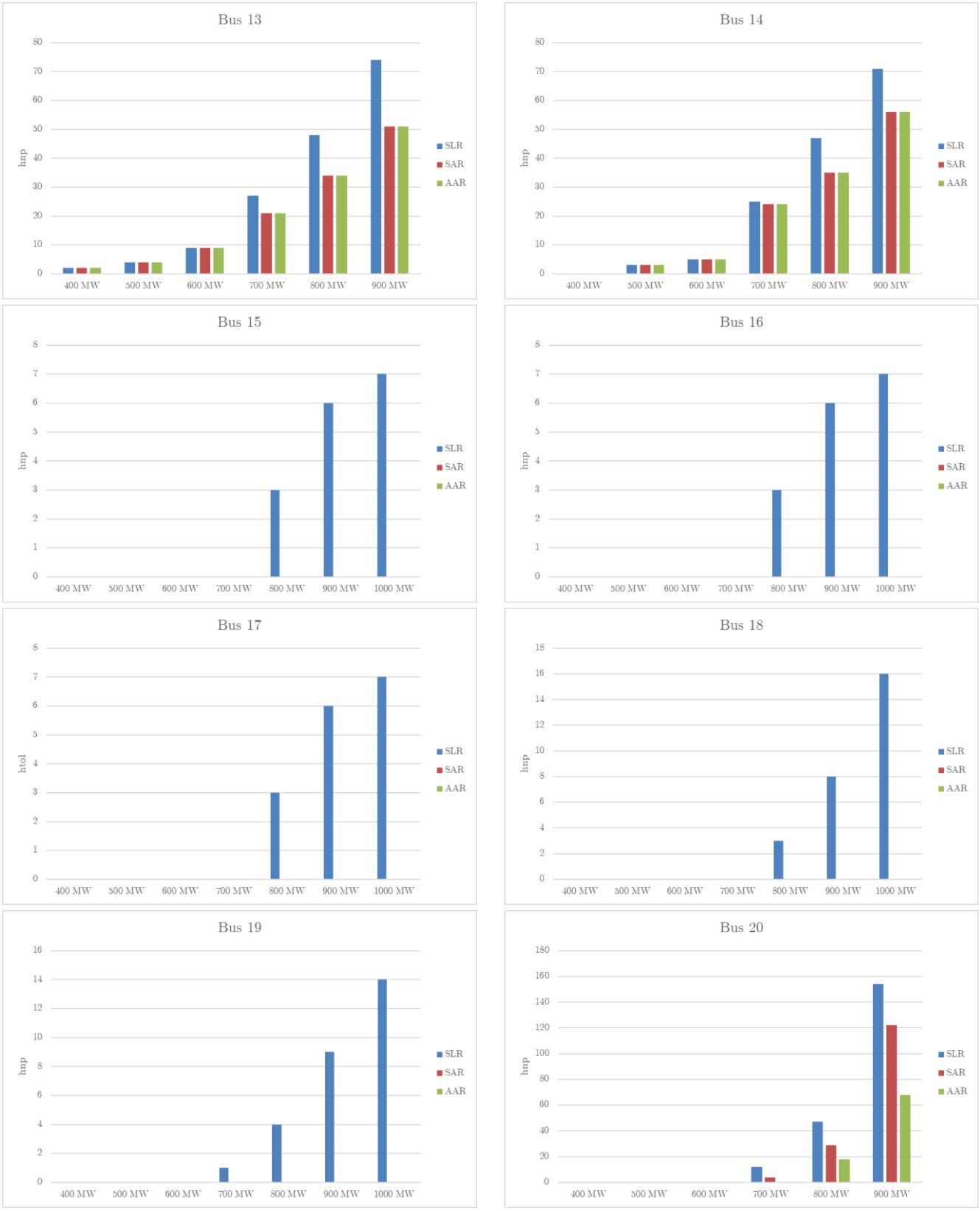

Figure 29: Comparison of h_{nP} for SLR, SAR and AAR at different injection levels

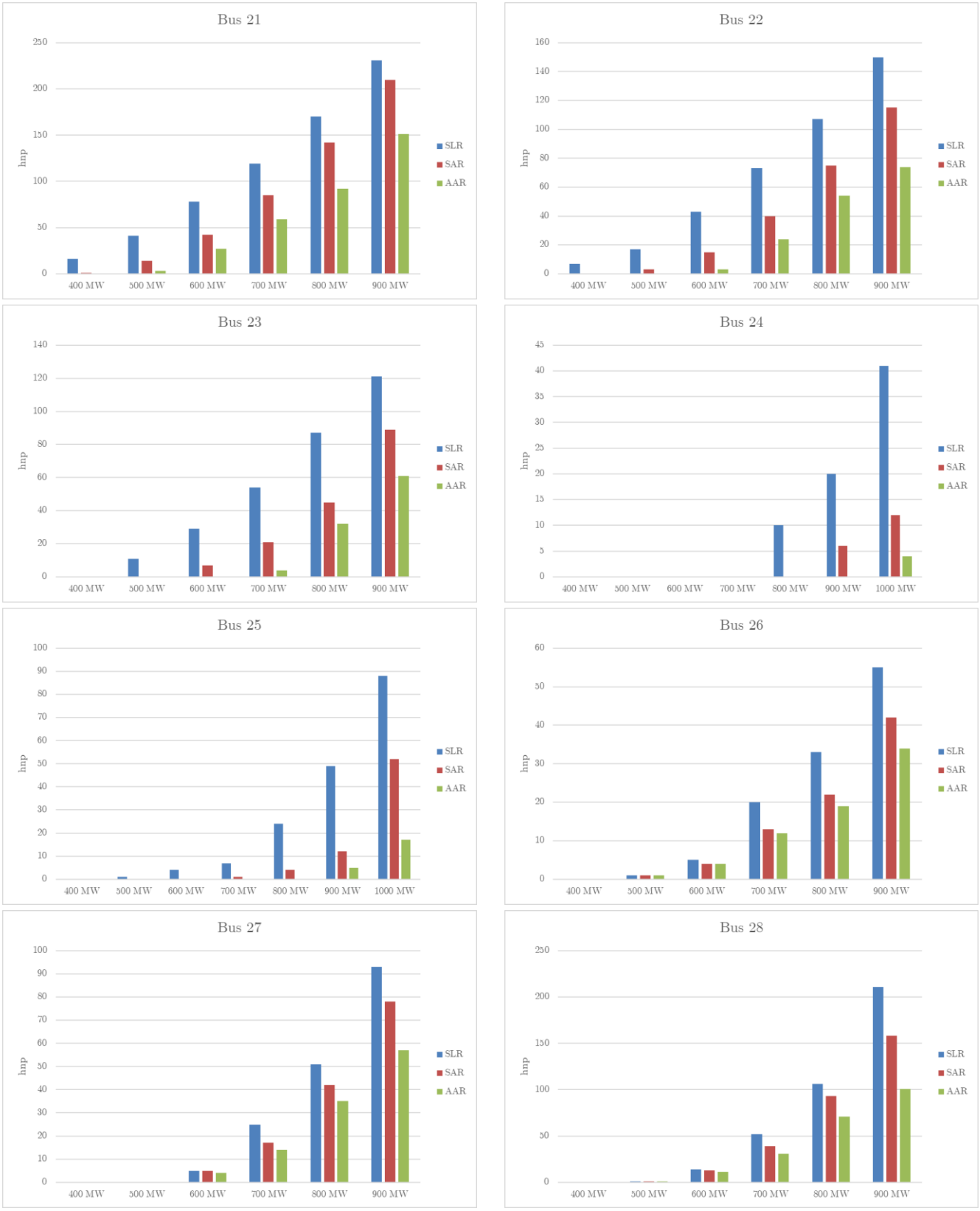

Figure 29: Comparison of h_{nP} for SLR, SAR and AAR at different injection levels

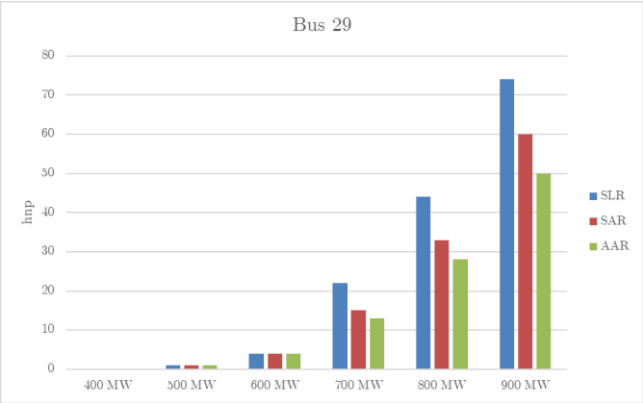

4.3 Impact of the tolerance h_{tol}

In section 4.1, the tolerance criterion $h_{tol} = 1\%$ was established to determine the hosting capacity of the nodes in the network. This section intends to show the impact of using different h_{tol} values, specifically a range of h_{tol} between 1% to 10% will be used, for the three rating adjustments considered. Table 13 summarizes the tolerance as a percentage $h_{tol_{\%}}$, and relative to a sample size of 288 hours h_{tol_m}, the equivalent hours relative to a full year are also included.

Table 13: Equivalent hours and tolerances in percentage and sample equivalent hours

$h_{tol_{\%}}$	1%	2%	3%	4%	5%	6%	7%	8%	9%	10%
h_{tol_m}	2	5	8	11	14	17	20	23	25	28
Hours/year	87	175	262	350	438	525	613	700	788	876

This sensitivity was analyzed independently for the three types of rating adjustment presented. The comparison was made by modifying the tolerance while maintaining the same rating adjustment. In this way, the direct impact on the hosting capacity of each node is shown under different reliability criteria.

Once again, it is necessary to emphasize that the impact of the sensitivities presented will depend on the particular conditions of each electrical system, therefore, it is not expected that all electrical systems present similar variations. The complementary analysis serves as guidelines regarding the conclusions that can be drawn from the information obtained when implementing this methodology, and possible additional applications of it.

4.3.1 Static line rating

Increasing the tolerance has a notorious impact on the buses that present greater restrictions to accepting additional power. Buses 5-14 present a hosting capacity of 400 MW based on $h_{tol} = 1\%$, increasing the tolerance to 2% or 3% increases said capacity by 100 MW, or even 200 MW for buses 5 and 14, for bus

8 the increase in hosting capacity reaches 300 MW. From a tolerance of 5%, the buses generally achieve an increase of 200 MW over the initial capacity. Increasing the tolerance beyond this point does not present significant or overall improvements to the ability to accommodate additional generation.

The most noticeable changes are observed for buses 15-19, all of them reach a capacity of 700 MW with a tolerance of 1%. By increasing the tolerance to 2%, the hosting capacity increases by 100 MW. The most substantial changes are observed with a tolerance of 3%, where the hosting capacity increases by 500 MW for nodes 15-17, while for node 18 the increase is 200 MW. By increasing the tolerance up to 5%, node 15 reaches a hosting capacity of 1,300 MW, while nodes 16 and 17 reach 1,500 MW.[1]

For the remaining nodes, the maximum increase in hosting capacity occurred with a tolerance of 5% to 6% and is 100 or 200 MW, this shows that high tolerance values do not necessarily equate to a significant change in the results. and they have the disadvantage of being too permissive for the proper reliability of an electrical system. It is expected that the results under an SLR scheme are more sensitive to tolerance because the transport capacity used for the operation is less.

Table 14 and Figure 30 show the complete results of the sensitivity analysis of the accommodation capacity vs. tolerance used.

Table 14: Hosting capacity at different tolerances h_{tol} - SLR

h_{tol} / Bus	Hosting capacity [MW]									
	1%	2%	3%	4%	5%	6%	7%	8%	9%	10%
1	400	400	400	400	400	500	500	500	500	500
2	700	800	800	900	900	900	1000	1000	1000	1000
3	600	700	700	800	800	900	900	900	900	900
4	700	800	900	1000	1000	1000	1000	1100	1100	1100
5	400	500	600	600	600	600	700	700	700	700
6	400	500	500	600	600	600	600	600	600	700
7	400	500	500	500	500	600	600	600	600	600
8	400	600	700	700	700	700	700	700	700	700
9	400	500	500	500	500	500	500	500	500	500
10	400	500	500	600	600	600	600	600	600	600
11	400	500	500	600	600	600	600	600	600	700
12	300	500	500	600	600	600	600	600	600	700
13	400	500	500	600	600	600	600	600	600	700
14	400	600	600	600	600	600	600	600	700	700
15	700	800	1200	1200	1300	1300	1300	1300	1300	1300

[1] 1500 MW was the maximum power considered

Bus \ h_{tol}	Hosting capacity [MW]									
	1%	2%	3%	4%	5%	6%	7%	8%	9%	10%
16	700	800	1200	1400	1500	1500	1500	1500	1500	1500
17	700	800	1200	1500	1500	1500	1500	1500	1500	1500
18	700	800	900	900	900	1000	1000	1000	1100	1100
19	700	800	800	900	1000	1100	1100	1200	1200	1200
20	600	600	600	600	700	700	700	700	700	700
21	300	300	300	300	300	400	400	400	400	400
22	300	300	400	400	400	500	500	500	500	500
23	400	400	400	500	500	500	500	500	500	500
24	700	700	700	800	800	800	900	900	900	900
25	500	600	700	700	700	700	700	700	800	800
26	500	600	600	600	600	600	700	700	700	700
27	500	600	600	600	600	600	600	600	700	700
28	500	500	500	500	600	600	600	600	600	600
29	500	600	600	600	600	600	600	700	700	700

Figure 30: Hosting capacity at different tolerances h_{tol} - SLR

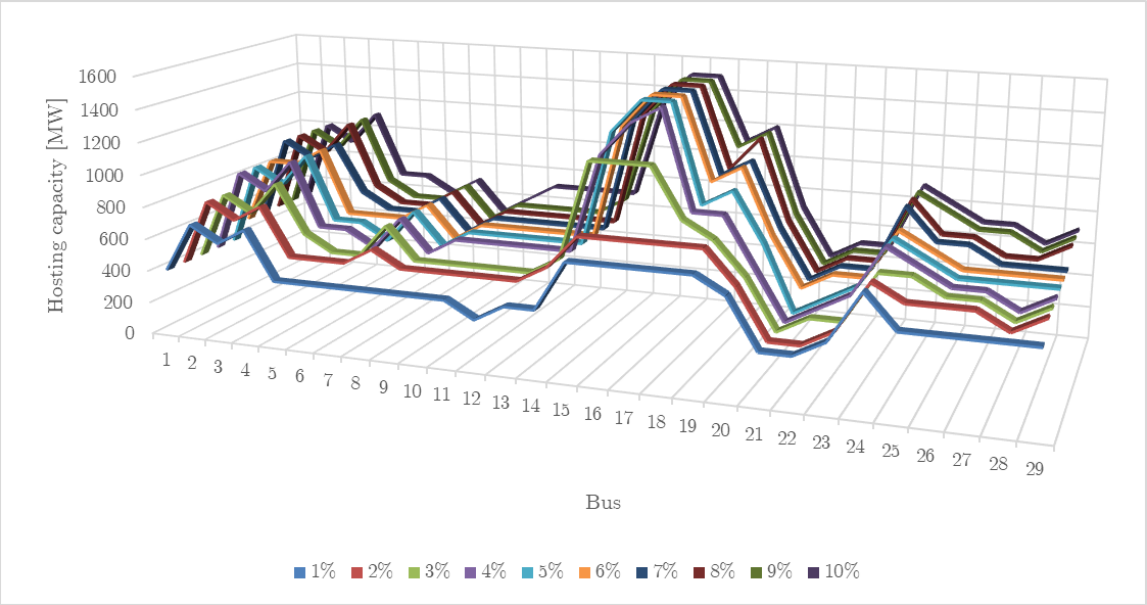

4.3.2 Seasonal adjustment rating

Considering SAR, nodes 5 to 14 reach a hosting capacity of 400 MW based on a tolerance of 1%. In general, the hosting capacity of these nodes grows by 200 MW considering a tolerance of 5%, while for nodes 8 and 12 the increase is 300 MW. By increasing the tolerance to 8%, the hosting capacity of nodes 8 and 12 grows by 400 MW. An impact similar to that presented in the case of SLR is observed.

Buses 15, 18 and 19 increase their hosting capacity to a lesser extent. This is because the capacity with a tolerance of 1% is high, being 1200 MW for bus 15

and 1100 MW for buses 18 and 19. For bus 15 the hosting capacity increases by 100 MW with tolerances of 2% to 7 %, and reaches 1400 MW with tolerances equal to or greater than 8%. As for buses 16 and 17, they already have a hosting capacity of 1,500 MW with a tolerance of 1%, so said capacity cannot be increased by contemplating looser tolerances.

As for the remaining buses, 20-29, the behavior is similar with increases between 100 MW to 200 MW by bringing the tolerance to 6%. For bus 23, it is observed that from a tolerance of 8% the hosting capacity grows by 300 MW compared to the capacity with a tolerance of 1%.

The global effect for initially constrained buses, in terms of their hosting capacity, is similar to that observed for an SLR criterion. However, it is observed that, for nodes with a high capacity to receive power, 15-19, the effects of considering looser tolerances are less, this is because the transport restrictions on these nodes are reduced, therefore, greater tolerances do not have a significant impact effect on the accommodation capacity

Table 15: Hosting capacity at different tolerances h_{tol} - SAR

h_{tol} / Bus	Hosting capacity [MW]									
	1%	2%	3%	4%	5%	6%	7%	8%	9%	10%
1	400	400	400	400	400	500	500	500	500	500
2	900	1000	1000	1000	1000	1000	1000	1000	1000	1000
3	800	900	900	900	900	1000	1000	1000	1000	1000
4	900	1100	1100	1100	1100	1100	1100	1100	1100	1100
5	400	500	600	600	600	700	700	700	700	800
6	400	500	500	600	600	600	700	700	700	700
7	400	500	600	600	600	600	600	700	700	700
8	400	600	700	700	700	700	700	800	800	800
9	400	500	500	500	500	500	500	500	500	600
10	400	500	500	600	600	600	600	600	700	700
11	400	500	500	600	600	600	600	700	700	700
12	300	500	500	600	600	600	600	700	700	700
13	400	500	500	600	600	600	600	700	700	700
14	400	600	600	600	600	600	600	600	700	700
15	1200	1300	1300	1300	1300	1300	1300	1400	1400	1400
16	1500	1500	1500	1500	1500	1500	1500	1500	1500	1500
17	1500	1500	1500	1500	1500	1500	1500	1500	1500	1500
18	1100	1100	1200	1200	1200	1200	1300	1300	1300	1300
19	1100	1200	1300	1300	1300	1300	1300	1400	1400	1400
20	600	700	700	700	700	700	700	700	700	700
21	400	400	400	400	500	500	500	500	500	500
22	400	500	500	500	500	600	600	600	600	600

Bus \ h_{tol}	Hosting capacity [MW]									
	1%	2%	3%	4%	5%	6%	7%	8%	9%	10%
23	500	500	600	600	600	600	600	700	700	700
24	800	800	900	900	1000	1000	1000	1000	1000	1000
25	700	800	800	800	900	900	900	900	900	900
26	500	600	600	600	700	700	700	800	800	800
27	500	600	600	600	600	700	700	700	700	700
28	500	500	500	500	600	600	600	600	600	600
29	500	600	600	600	600	700	700	700	700	700

Figure 31: Hosting capacity at different tolerances h_{tol} - AAR

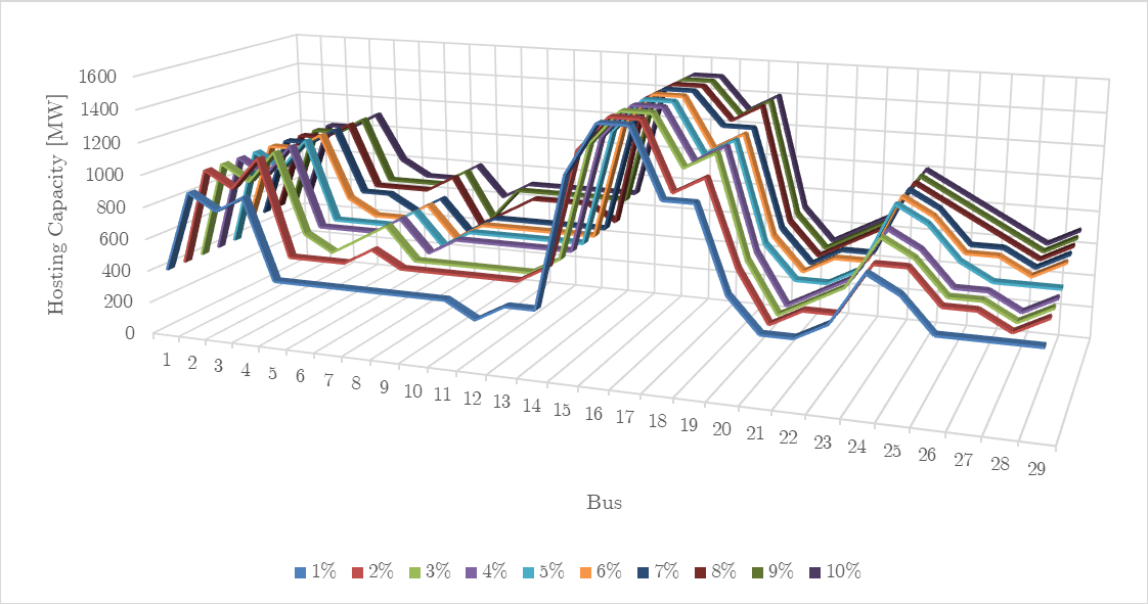

4.3.3 Ambient adjustment rating

The changes when increasing the tolerance under AAR criteria are similar to those presented in sections 4.3.1 and 4.3.2. In general, the increases to the hosting capacity are approximately 100 to 200 MW when considering a tolerance of 5%. For tolerances greater than 6%, the increases reach 200 MW or 300 MW, except for bus 8 where the increase in hosting capacity is 400 MW for looser tolerances. For buses 1, 3, 9, 18, 20, 23, 24 and 28 the increase is only 100 MW, this can be attributed to the rapid increase in the number of overload scenarios when increasing power additions beyond 700 MW.

Table 16: Hosting capacity at different tolerances h_{tol} - AAR

Bus \ h_{tol}	Hosting capacity [MW]									
	1%	2%	3%	4%	5%	6%	7%	8%	9%	10%
1	400	400	400	500	500	500	500	500	500	500
2	1000	1000	1000	1000	1000	1000	1000	1000	1000	1000
3	900	1000	1000	1000	1000	1000	1000	1000	1000	1000
4	900	1000	1000	1000	1100	1100	1100	1100	1100	1100

Bus \ h_{tol}	Hosting capacity [MW]									
	1%	2%	3%	4%	5%	6%	7%	8%	9%	10%
5	400	500	600	600	600	700	700	700	700	800
6	400	500	500	600	600	600	700	700	700	700
7	400	500	600	600	600	600	600	700	700	700
8	400	600	700	700	700	800	800	800	800	800
9	500	500	500	500	500	600	600	600	600	600
10	400	500	500	600	600	600	600	600	700	700
11	400	500	500	600	600	600	600	700	700	700
12	300	500	500	600	600	600	600	700	700	700
13	400	500	500	600	600	600	600	700	700	700
14	400	600	600	600	600	600	600	600	700	700
15	1200	1300	1300	1300	1300	1300	1300	1400	1400	1400
16	1500	1500	1500	1500	1500	1500	1500	1500	1500	1500
17	1500	1500	1500	1500	1500	1500	1500	1500	1500	1500
18	1200	1200	1200	1300	1300	1300	1300	1300	1300	1300
19	1300	1400	1400	1400	1400	1400	1400	1400	1400	1500
20	700	700	700	700	700	700	800	800	800	800
21	400	500	500	500	500	500	500	500	500	600
22	500	600	600	600	600	600	600	600	700	700
23	600	700	700	700	700	700	700	700	700	700
24	900	1000	1000	1000	1000	1000	1000	1000	1000	1000
25	800	900	900	900	900	1000	1000	1000	1000	1000
26	500	600	600	600	700	700	800	800	800	800
27	500	600	600	600	700	700	700	700	700	700
28	500	500	500	600	600	600	600	600	600	600
29	500	600	600	600	700	700	700	700	700	800

Figure 32: Hosting capacity at different tolerances h_{tol} - AAR

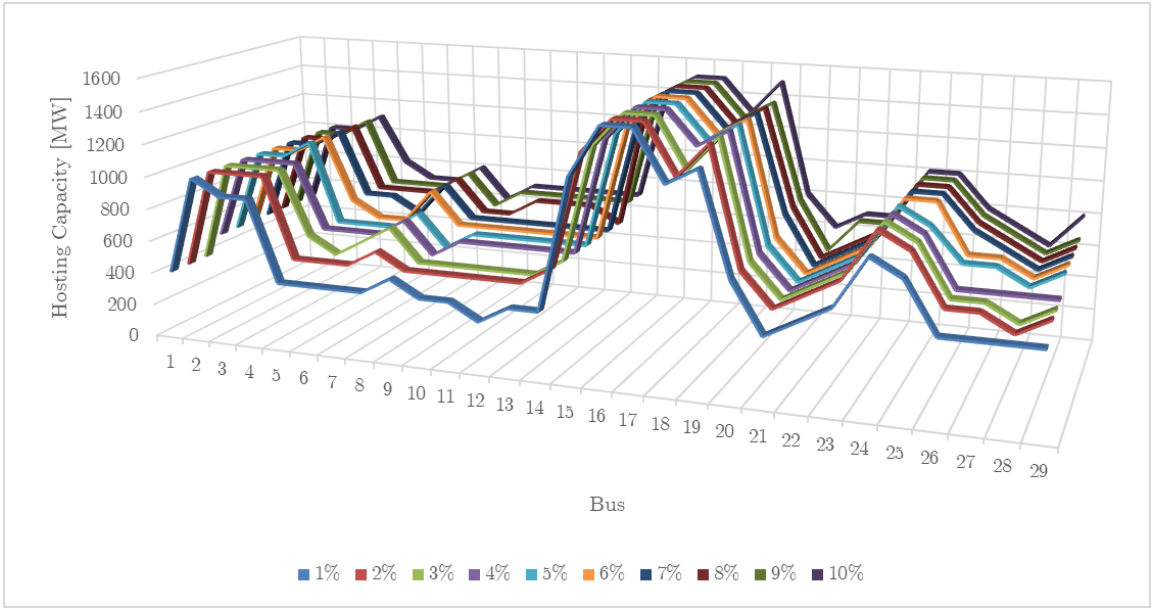

4.4 Critical elements in the grid

An additional result of the methodology is the possibility of identifying the elements of the system that present overloads more frequently, or the contingencies that usually limit the power additions in the system. This makes it possible to identify potential regions for improvement to plan investments in the transmission network.

In this analysis, it is feasible to identify the components most vulnerable to overloads during a contingency after including additional power injections. To demonstrate the process, the results from the addition of 900 MW are used, while comparing the use of adjustment factors SLR, SAR, and AAR.

Table 17 and Figure 33 present specifics on transmission lines at risk of overloading and quickly reveal the limiting elements in the network with a power increase. The transmission line between buses 16 and 21 has the higher number of overloading events after a contingency. Combining Table 17 and Table 18 it can be seen that the overloading of one of the lines between these buses is a direct result of the contingency of its parallel circuit. This behaviour is similar for the links between buses 8-9, when the overloading occurs, usually as a consequence of the disconnection of its parallel element.

In addition to identifying overloaded elements, it is possible to indicate limiting contingencies for adding power to the system. This analysis helps to identify which network elements reduce transmission system sufficiency. Table 18 and Figure 34 provide details on critical and limiting contingencies for adding 900 MW, considering three transmission capacity estimates.

Table 17: Overloaded elements and number of events – Addition 900 MW

Overloaded element			Overloading events		
Bus 1	Bus 2	ID	SLR	SAR	AAR
7	8	A	341	320	266
8	9	B	179	138	77
12	13	A	215	234	136
16	21	B	493	408	284
2	25	B	42	10	5
26	28	B	160	118	68
1	2	B	194	163	121
5	6	A	81	60	60
20	19	B	255	122	68
10	13	A	251	204	204
10	11	B	6	2	0
6	11	B	12	0	0

Overloaded element			Overloading events		
Bus 1	Bus 2	ID	SLR	SAR	AAR
4	14	A	7	0	0
3	18	C	2	0	0
9	39	B	5	0	2
3	4	B	11	4	0
16	19	B	2	0	0
4	5	A	34	22	22
13	14	A	90	68	68
1	39	B	54	46	43
14	15	B	56	52	52
26	29	B	17	18	15
17	27	B	124	102	75
26	27	B	119	100	84
22	23	B	5	6	2
14	15	A	4	4	4
25	26	B	9	2	0
22	23	A	18	6	0

Figure 33: Overloaded elements and number of events – Addition 900 MW

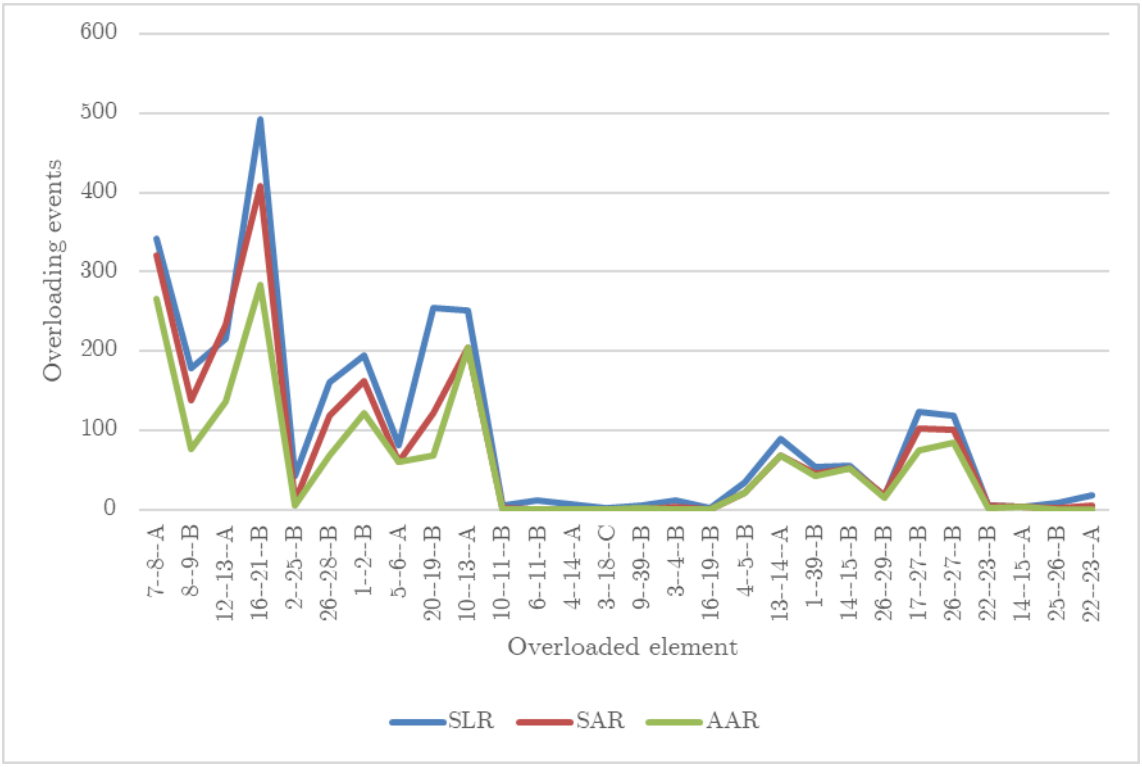

Table 18: Critical contingencies and number of overloading events – Addition 900 MW

Contingency		Overloading events		
Bus 1	Bus 2	SLR	SAR	AAR
6	7	169	193	192
8	9	179	138	77
12	11	215	234	136
16	21	493	408	284
2	25	42	10	5
26	28	160	118	68
1	2	194	163	121
5	6	120	76	69
13	14	107	78	78
20	19	255	122	68
4	5	341	272	272
10	11	6	2	0
6	11	12	0	0
3	18	2	0	0
9	39	5	0	2
3	4	11	4	0
16	19	2	0	0
5	8	67	55	9
1	39	54	46	43
14	15	56	52	52
26	29	17	18	15
17	27	124	102	75
26	27	119	100	84
22	23	5	6	2
4	14	4	4	4
25	26	9	2	0
16	24	18	6	0

Figure 34: Critical contingencies and number of overloading events – Addition 900 MW

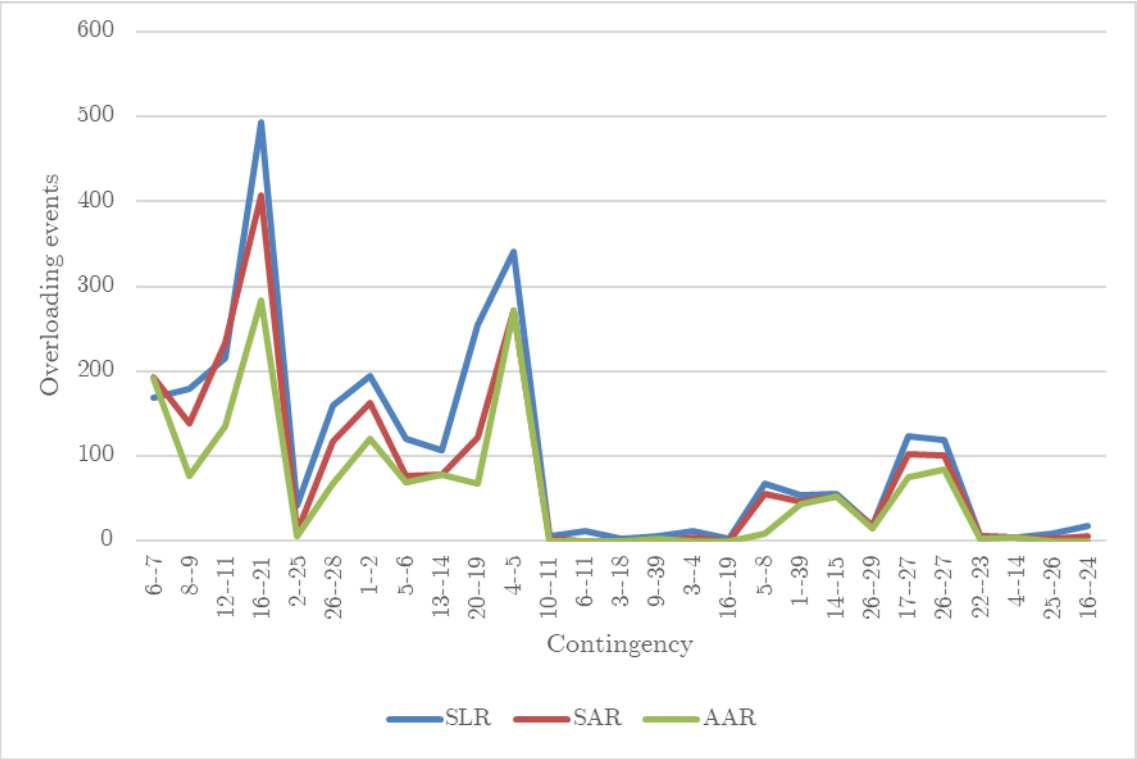

Regarding the expansion criteria, optimization ones are usually followed. The results obtained through the implementation of this methodology do not represent the most economical expansions for the transmission network. However, the aforementioned results can serve as an indicator of candidate projects for long-term expansions. These candidates undergo an optimization process following the criteria established in the planning methodology for each system.

4.5 SAR and AAR impact on overload seasonality

Another set of results obtainable from implementing the methodology is to identify the patterns in the temporality of the overloads registered in the system. This may be relevant to contrast and establish a possible correlation of these events with consumption patterns or with patterns in the generation behaviour. It is expected that when considering seasonal and hourly adjustments in the transmission capacity, the temporality of the overloads or restrictions in the grid will change. To show this, the scenarios with overloads for each month of the year will be compared under different rating adjustment factors.

As described in section 3.2, demand and generation present seasonal behavior. Regarding the demand, it was observed that it tends to increase in the winter months. Under a static rating scheme, it is expected that during these months the greatest number of overloads or congestions will be recorded in the network. The variable schemes used, SAR and AAR, consider that in these months the

transport capacity increases by approximately 10% relative to the reference capacity in summer, or up to 20% for the monthly effect of the season and nighttime.

To make it easier to compare, the percentage contribution of each month to the number of overloads recorded for each power level P_n is shown. The effect of using variable ratings on the seasonality of the registered overloads is identified under a common reference.

From the graphs in Figure 35 to Figure 40 a clear pattern can be observed, when considering a static limit, the overloads are distributed throughout the year, while with SAR and AAR factors the overloads are predominant in the summer months, when the line rating is lower. The most extreme behavior is observed in the range from 400 MW to 600 MW, for which with a static limit the distribution is relatively uniform for the months of January, February, December and August. On the contrary, when using the seasonal adjustment, the overloads occur mostly in the month of August, compared to the other months. This behavior is accentuated when using the AAR factor.

This result does not seem to have much relevance for the calculation of the hosting capacity; however, it is a possible tool to identify the time, or month of the year, in which it is more likely to resort to curtailments of the new plants due to congestion in the transmission grid. This section shows that it is possible to obtain additional information with practical applications using the results obtained from the implementation of this methodology.

Figure 35: Comparison of monthly contributions to h_{nP}, addition 400 MW

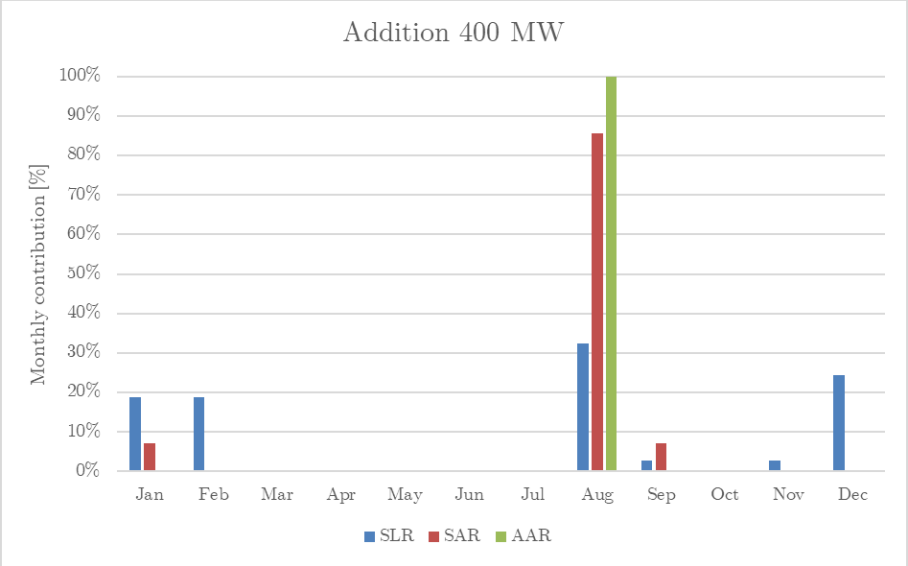

Figure 36: Comparison of monthly contributions to h_{nP}, addition 500 MW

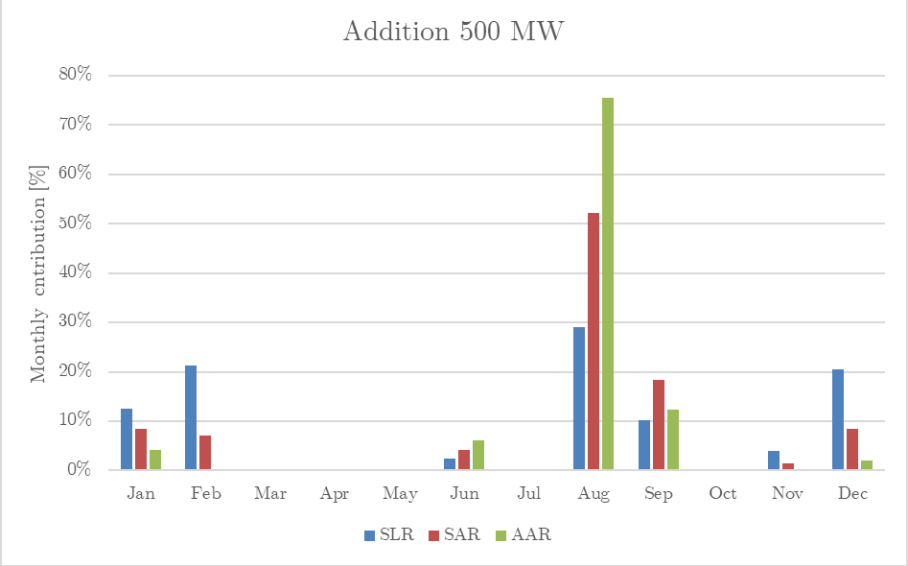

Figure 37: Comparison of monthly contributions to h_{nP}, addition 600 MW

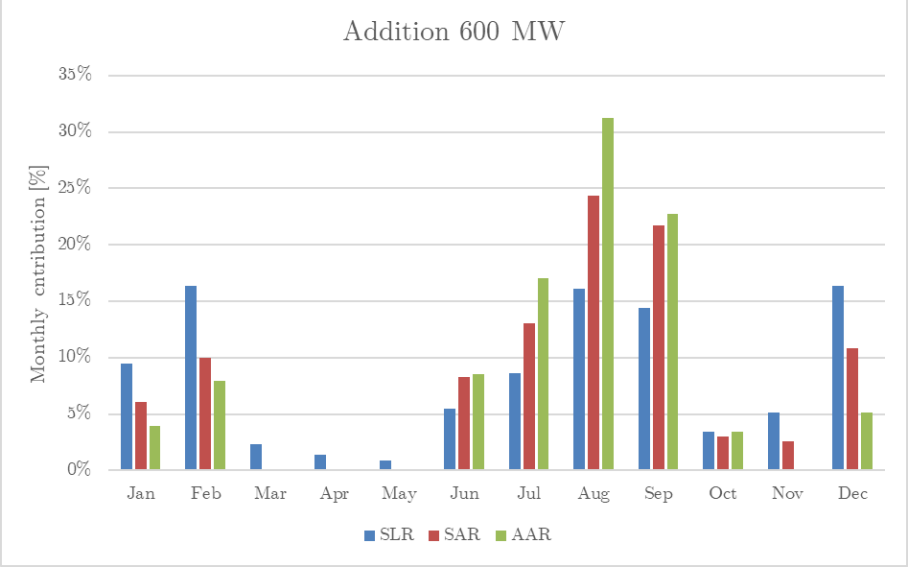

Figure 38: Comparison of monthly contributions to h_{nP}, addition 700 MW

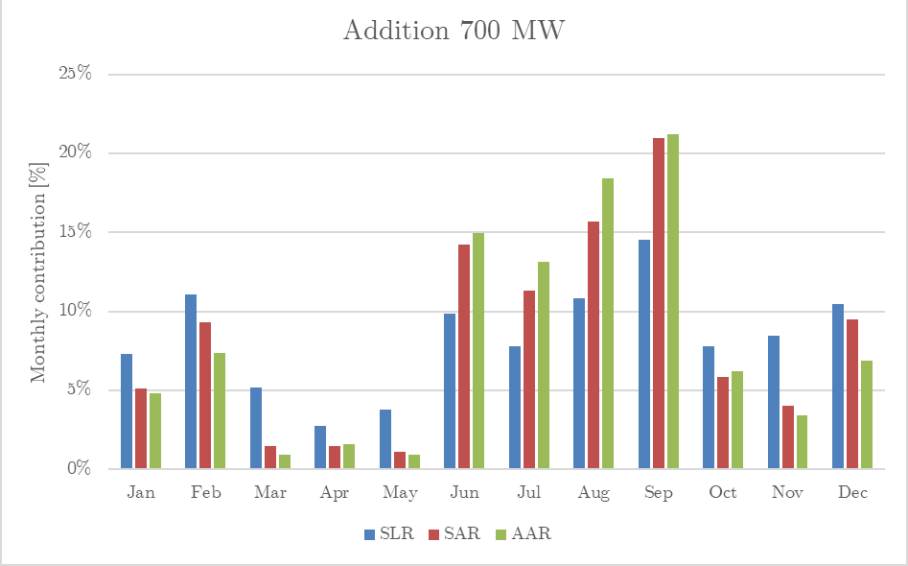

Figure 39: Comparison of monthly contributions to h_{nP}, addition 800 MW

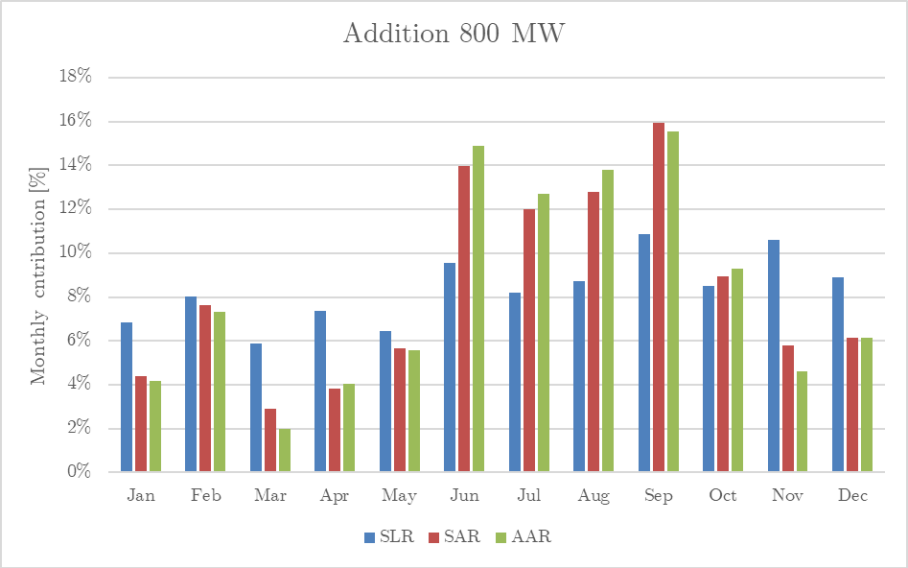

Figure 40: Comparison of monthly contributions to h_{nP}, addition 900 MW

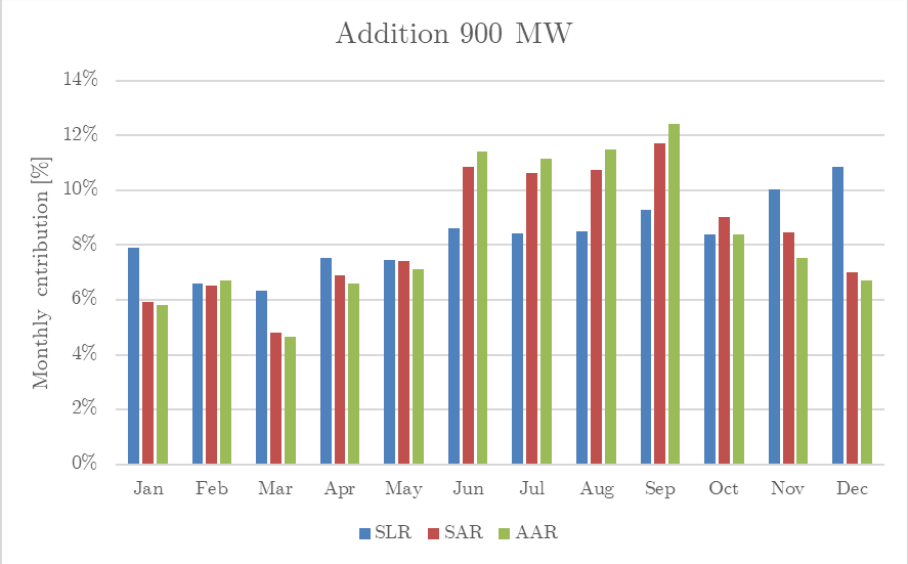

5 Conclusions

5.1 Design and application of the methodology

After the development and implementation of the methodology, it is possible to identify the strengths of the methodology. The initial objective of this work, which was to identify the capacity of a transmission node to allocate additional power, has been achieved.

The sampling methodology accurately represents the operation of the system, and it is possible to adjust the sampling to represent the typical operation of the particular system being analyzed. The sampling process was performed using historical information on system operation, but it is possible to use the dispatch results of the optimization tools designed to simulate the combined operation of the elements in the system to meet demand at the lowest possible cost. This is an advantageous aspect of the methodology, since the source of the analysis scenarios is flexible, and therefore it is possible to adapt the methodology to specific needs.

Three criteria were used to adjust the carrying capacity. One criterion, where the carrying capacity is unique for all analysis scenarios, is called Static Line Rating (SLR). The second criterion used is an improvement based on the average conditions of each season of the year, this second adjustment is called Seasonal Adjustment Rating (SAR). Finally, an adjustment factor is used that is based on the average environmental conditions with hourly resolution for each month of the year, this is called Ambient Adjustment Rating (AAR) and is a substantial improvement to estimate more accurately the carrying capacity of the transmission elements without the computational effort and collection of real-time information for the dynamic adjustment of the carrying capacity, or Dynamic Line Rating (DLR).

Regarding the allocation capacity, it is strongly influenced by the transport capacity adjustment factors, since the consideration of more realistic environmental conditions tends to increase the transport capacity of the elements in the network. In terms of results, for certain network nodes, the effect of using AAR compared to SAR and SLR represents an additional 200 to 800 MW in the capacity of that node to allocate additional power. These results are clearly dependent on the network topology and the tolerance used in the decision criteria as mentioned in sections 3.1, 4.1, and 4.3.

The following figure, which is the same as Figure 28, summarizes the main result of the implementation of the methodology. It shows in a more direct way

the comparison of the results mentioned in the previous paragraph, where the improvements from implementing more accurate estimates of transport capacity are substantial.

Figure 41: Hosting capacity for $h_{tol_{\%}} = 1\%$

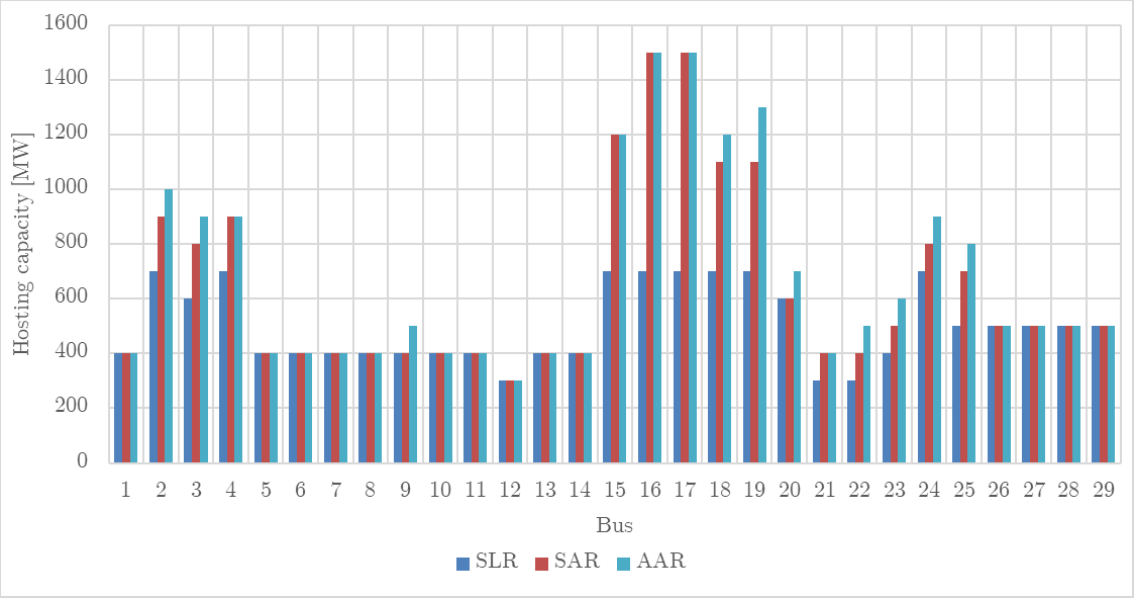

In addition to increasing the additional power capacity that a node can allocate; the implementation of SAR and AAR adjustment factors shows significant improvements in the number of overloads recorded in the simulations. Section 4.2 shows in detail the impact of the adjustment factors on the amount of congestion h_{np} recorded at the different levels of additional power used in the tests.

The tolerance, h_{tol}, also has a significant impact on the ability of a node to accept additional power. Section 4.3 details the effect of reducing the constraint on the tolerance. While it is true that increased transport capacity is observed by having more flexibility in h_{tol}, there are drawbacks to taking this action. The main disadvantage is underestimating the risk of overloading or undesirable conditions. In addition, the tolerance is usually strict according to the applicable regulation for each system, in order to reduce the impact of N-1 contingencies on the system.

In general, determining the capacity of a node to allocate new power is a necessary task to know the real capacity of the network to incorporate additions to the generation park, which has a medium- and long-term impact on the operation of the system, since a network with greater constraints will be equivalent to higher operating costs for the system. The efficiency of larger power plants in a network with transmission capacity has been studied and are current planning criteria, even considering the increase in smaller distributed generation.

An improvement in the estimation of hosting capacity, such as the one developed in this work, allows us to meet the regulatory and economic requirements for modern transmission systems. Increasing the utilization of assets in the transmission system has benefits in the economic efficiency of large power systems. In addition, a system with higher utilization allows reducing the number of additional elements required to be incorporated into the transmission network, which leads to logistical benefits for transmission companies, since the development of projects of this type is usually associated with a high impact on area close to the projects.

5.2 Possible applications

The developed methodology has a wide field of application in the operation of electric power systems and even in the development of public policies related to the electricity sector. Initially, the methodology was designed to serve as a basic indicator to determine whether the interconnection of a generating plant is feasible without the need to reduce its expected production due to constraints in the transmission network.

According to this description, it is expected to be useful in the planning of system expansions, helping planners to determine the optimal location, within the feasible options, and the capacity of new facilities to ensure the safe growth of the system.

Another context is the use of the methodology to identify the integration of renewable energy. A similar tool can be useful to determine the transmission capacity available to inject energy into the system, ensuring an adequate and stable integration of these variable sources. The correlation of environmental conditions with the average production patterns of variable renewable power plants is also taken into account. It is possible to establish a direct relationship between the parameters.

The methodology also allows to evaluate, in a more precise way, the capacity of the system to recover in the event of contingencies or large-scale disturbances. This is useful to quantify the resilience of the system to adverse situations in a medium- or long-term horizon.

6 Bibliography

[1] A. Arroyo, P. Castro, R. Martinez, M. Manana, A. Madrazo, R. Lecuna and A. Gonzalez, "Comparison between IEEE and CIGRE thermal behaviour standards and measured temperature on a 132-kV overhead power line," *Energies,* vol. 8, p. 13660–13671, 2015.

[2] P. Van Staden and J. A. De Kock, "The practical comparison of conductor operating temperatures against IEEE and CIGRE ampacity calculations," in *IEEE Power and Energy Society Conference and Exposition in Africa: Intelligent Grid Integration of Renewable Energy Resources (PowerAfrica)*, 2012.

[3] CIGRE, "Thermal behaviour of overhead conductors," *WG 22.12,* 2002.

[4] IEEE, "IEEE Standard for Calculating the Current-Temperature of Bare Overhead Conductors," *IEEE Std 738-1993,* pp. 1-48, 1993.

[5] V. T. Morgan, "The thermal rating of overhead-line conductors Part I. The steady-state thermal model," *Electric power systems research,* vol. 5, p. 119–139, 1982.

[6] W. Z. Black and W. R. Byrd, "Real-Time Ampacity Model for Overhead Lines," *IEEE Transactions on Power Apparatus and Systems,* Vols. PAS-102, pp. 2289-2293, 1983.

[7] N. P. Schmidt, "Comparison between IEEE and CIGRE ampacity standards," *IEEE Transactions on Power Delivery,* vol. 14, pp. 1555-1559, 1999.

[8] W. Z. Black and R. L. Rehberg, "Simplified Model for Steady State and Real-Time Ampacity of Overhead Conductors," *IEEE Transactions on Power Apparatus and Systems,* Vols. PAS-104, pp. 2942-2953, 1985.

[9] M. Bartos, M. Chester, N. Johnson, B. Gorman, D. Eisenberg, I. Linkov and M. Bates, "Impacts of rising air temperatures on electric transmission ampacity and peak electricity load in the United States," *Environmental Research Letters,* vol. 11, p. 114008, 2016.

[10] Y.-Q. Ding, M. Gao, Y. Li, T.-L. Wang, H.-L. Ni, X.-D. Liu, Z. Chen, Q.-H. Zhan and C. Hu, "The effect of calculated wind speed on the capacity of dynamic line rating," in *2016 IEEE International Conference on High Voltage Engineering and Application (ICHVE)*, 2016.

[11] V. T. Morgan, "The thermal rating of overhead-line conductors part II. A sensitivity analysis of the parameters in the steady-state thermal model," *Electric power systems research,* vol. 6, p. 287–300, 1983.

[12] T. O. Seppa, "A practical approach for increasing the thermal capabilities of transmission lines," *IEEE Transactions on Power Delivery,* vol. 8, p. 1536–1550, 1993.

[13] P. J. M. Interconnection, *Guide for determination of bare overhead transmission conductors,* 2022.

[14] D. A. Douglass, J. Gentle, H.-M. Nguyen, W. Chisholm, C. Xu, T. Goodwin, H. Chen, S. Nuthalapati, N. Hurst, I. Grant and others, "A review of dynamic thermal line rating methods with forecasting," *IEEE Transactions on Power Delivery,* vol. 34, p. 2100–2109, 2019.

[15] 1. CIGRE Working Group B2., Guide for selection of weather parameters for bare overhead conductor ratings, CIGRE, 2006.

[16] Federal Electricity Regulatory Comission, "FERC Order 881," FERC, 2021.

[17] D. R. Swatek, "An expected per-unit rating for overhead transmission lines," *International journal of electrical power & energy systems,* vol. 26, p. 241–247, 2004.

[18] K. W. Cheung, "FERC Order 881-A Step Towards Dynamic Line Ratings for Improved Market Efficiency," in *2022 IEEE PES 14th Asia-Pacific Power and Energy Engineering Conference (APPEEC)*, 2022.

[19] J. D. Glover, M. S. Sarma and T. Overbye, Power system analysis & design, SI version, Cengage Learning, 2012.

[20] A. J. W. B. F. Wollenberg and G. B. Sheblé, Power generation, operation, and control, 2014.

[21] O. H. Barda, J. Dupuis and P. Lencioni, "Multicriteria location of thermal power plants," *European Journal of Operational Research,* vol. 45, p. 332–346, 1990.

[22] B. G. Gorenstin, N. M. Campodonico, J. P. Costa and M. V. F. Pereira, "Power system expansion planning under uncertainty," *IEEE Transactions on Power Systems,* vol. 8, pp. 129-136, 1993.

[23] N. I. Voropai and E. Y. Ivanova, "Multi-criteria decision analysis techniques in electric power system expansion planning," *International journal of electrical power & energy systems,* vol. 24, p. 71–78, 2002.

[24] A. Bejan, A. Almerbati and S. Lorente, "Economies of scale: The physics basis," *Journal of Applied Physics,* vol. 121, 2017.

[25] L. R. Christensen and W. H. Greene, "Economies of scale in US electric power generation," *Journal of political Economy,* vol. 84, p. 655–676, 1976.

[26] D. L. Phung, "Theory and evidence for using the economy-of-scale law in power plant economics," 1987.

[27] New England ISO, "Regional System Planning Process," 2023.

[28] New England ISO, "Methodology Document for the Assessment of Transfer Capability," 2016.

[29] New England ISO, "Transmission Planning Process Guide," 2023.

[30] New England ISO, "Transmission Planning Technical Guide," 2023.

[31] A. Chowdhury and D. Koval, Power distribution system reliability: practical methods and applications, John Wiley & Sons, 2011.

[32] R. Billinton and R. N. Allan, Reliability assessment of large electric power systems, Springer Science & Business Media, 2012.

[33] G. F. Kovalev and L. M. Lebedeva, Reliability of power systems, vol. 1, Springer, 2019.

[34] S. B. Aruna, D. Suchitra, R. Rajarajeswari and S. G. Fernandez, "A comprehensive review on the modern power system reliability assessment," *International Journal of Renewable Energy Research (IJRER),* vol. 11, p. 1734–1747, 2021.

[35] Comisión Reguladora de Energía Eléctrica, *Norma Técnica de Calidad de Transmision,* 2017.

[36] M. Papic, M. Clemons, S. Ekisheva, J. Langthorn, T. Ly, M. Pakeltis, R. Quest, J. Schaller, D. Till and K. Weisman, "Transmission availability data system (TADS) reporting and data analysis," in *2016 International Conference on Probabilistic Methods Applied to Power Systems (PMAPS)*, 2016.

[37] North American Electric Reliability Corporation, "2023 State of Reliability Technical Assessment," NERC, 2023.

[38] North American Electric Reliability Corporation, "2012 State of Reliability Technical Assessment," NERC, 2012.

[39] P. Kundur, "Power system stability," *Power system stability and control,* vol. 10, p. 7–1, 2007.

[40] North American Electric Reliability Corporation, *Standard 51 — Transmission System Adequacy and Security,* 2022.

[41] ENTSO (European Network of Transmission System Operators for Electricity), *P3 – Policy 3: Operational Security,* 2009.

[42] Comisión Reguladora de Energía Eléctrica, *Norma Técnica de Programación de la Operación,* 2020.

[43] Texas A&M University, "New England IEEE 39-Bus System," Electric Grid Case Repository, 2016. [Online]. Available: https://electricgrids.engr.tamu.edu/electric-grid-test-cases/new-england-ieee-39-bus-system/. [Accessed 2022].

[44] Siemens Power Technologies International, "PSS®E Program Operation Manual," Siemens, Schenectady, NY, 2022.

[45] Siemens Power Technologies International, "Program Application Guide Volume 1," Siemens, Schenectady, NY, 2022.